FATIGUE BEHAVIOR OF FLAX FIBER REINFORCED POLYMER MATRIX COMPOSITES

A Thesis
Submitted to the Graduate Faculty
of the
North Dakota State University
of Agriculture and Applied Science

By

Md. Zahirul Islam

In Partial Fulfillment of the Requirements
for the Degree of
MASTER OF SCIENCE

Major Department:
Mechanical Engineering

October 2019

Fargo, North Dakota

North Dakota State University
Graduate School

Title

Fatigue Behavior of Flax Fiber Reinforced Polymer Matrix Composites

By

Md. Zahirul Islam

The Supervisory Committee certifies that this ***disquisition*** complies with North Dakota State University's regulations and meets the accepted standards for the degree of

MASTER OF SCIENCE

SUPERVISORY COMMITTEE:

Dr. Chad Ulven
Chair

Dr. Alan Kallmeyer

Dr. Dean Webster

Dr. Xiangfa Wu

Dr. Md. Saidal Borhan

Approved:

11/8/19
Date

Dr. Alan Kallmeyer
Department Chair

ABSTRACT

Bio-based flax fiber polymer composites (FFPC) have the potential to replace metals and synthetic fibers in certain applications due to their unique mechanical properties. However, the long term reliability of FFPC needs to be better understood. In this study, the fatigue limit was evaluated using mathematical, thermographic, and energy-based approaches. Each approach determined fatigue limits around 45% load of ultimate tensile strength at a loading frequency of 5 Hz. Thermographic and energy-based approaches were also implemented at different loading frequencies (5, 7, 10, and 15 Hz) to define the effect of loading frequency on the fatigue life. Fatigue limit was found to decrease slowly with increasing loading frequency. Moreover, two forms of damage energy (thermal and micro-mechanical) during cyclic loading was separated using an experimental approach to pinpoint the main responsible damage energy for decreasing fatigue limit with increasing loading frequency.

ACKNOWLEDGEMENTS

I would like to express my sincere gratitude to my Creator, my parents, my sister, and all other individuals from whom I got help, support, and encouragement throughout my journey of the life of 29 years. I would like to express special gratefulness to my supervisor Dr. Chad Ulven for being a great mentor through my journey of Master's at NDSU. I also would like to thank all of my group members, faculty and staff of Mechanical Engineering department, NDSU for helping to do study and research over last two years. I would like to be grateful to CSMS, NDEPSCoR to provide funding for my study and research. I also would like to be thankful to all of my committee members for their time, kindness, suggestion, idea, and effort to make my current dissertation better.

I believe, this page is so small to mention the name of all the individuals to whom I would like to be grateful, but I should hold their name in my memory and prayer.

DEDICATION

In the name of Allah, who created me.

TABLE OF CONTENTS

LIST OF TABLES

LIST OF FIGURES

LIST OF ABBREVIATIONS

UTS .....Ultimate Tensile Strength.

HCFS.....High Cycle Fatigue Strength.

VARTM .....Vacuum Assisted Resin Transfer Molding.

LIST OF SYMBOLS

F .....Force, N

f .....Loading frequency, Hz

s .....Elongation, m

ρ.....Density of sample, kg/ m^3

c.....Specific heat of sample, J/kg ˚C

T .....Temperature of the sample, ˚C

t .....Time, sec.

V.....Volume of the sample, m^3

T_g .....Glass transition temperature, ℃

N_f .....Fatigue life, Cycle required to failure.

E_T (per unit time).....Total dissipated energy per unit time, J/(m^3.sec)

E_T (per cycle).....Total dissipated energy per cycle, J/(m^3.cycle)

$H_{cd+cv+ir}$ (per unit time) .....Heat energy transferred from the sample by conduction, convection, and radiation, J/(m^3.sec)

$H_{cd+cv+ir}$ (per cycle) .....Heat energy transferred from the sample by conduction, convection, and radiation, J/(m^3.cycle)

E_d (per unit time).....Energy responsible for damage creation within the sample, J/(m^3.sec)

E_d (per cycle).....Energy responsible for damage creation within the sample, J/(m^3.cycle)

1. INTRODUCTION

1.1. Background

Fiber-reinforced polymer matrix composites have a wide range of applications in the sectors of automotive, aerospace, sports equipment, among others, due to their high specific strength, stiffness as well as reduced weight. In addition to those favorable properties, bio-composites also have eco-friendliness and improved bio-degradability [1]. Despite these advantages, the applications of bio-composites are still limited due to a lack of knowledge regarding their long term reliability under fluctuating loads. Though many studies have been conducted to define the long term reliability of metals and synthetic fiber reinforced composites through fatigue testing, very few studies have focused on the long term reliability of natural fiber reinforced composites.

Fatigue failure is a process of gradual cumulative damage accumulation within materials over time. Fatigue failure generally consists of three stages: (i) Crack initiation, (ii) crack propagation, and (iii) final failure [2]. The total life span spent on those stages are not same for metals compared to composite materials. For a homogeneous materials like steel, the damage accumulation rate is slow at the beginning, therefore the crack initiation occurs only after a significant portion of the fatigue lifespan. After a certain number of fatigue cycles, a single crack initiates and propagates perpendicular to the loading axis to evoke final failure. However, the mechanism of crack initiation and propagation are somewhat more complex in the case of composite materials. Within composite materials, cracks initiate from different locations at the beginning of their fatigue life. These cracks can initiate either in the matrix or interface between the fiber and matrix. In the case of composite materials, the crack initiates rapidly at the beginning

of the fatigue life and grows steadily and slowly during the entire propagation stage; the crack/damage again grows rapidly just before the final stage of failure [3-5].

The fatigue life of a polymer matrix composite depends on fiber architecture, fiber type, fiber orientation, volume fraction of the fiber, and fiber-matrix adhesion. The effect of fiber architectures on fatigue properties of flax fiber reinforced composites were investigated by Bensadon [6]. Moreover, natural fiber reinforced composite materials show significantly different properties from synthetic fiber reinforced composites under dynamic loading [7]. Unlike conventional fibers, which are more or less elastic in nature, natural fibers are themselves viscoelastic in nature [8]. Viscoelastic properties of both fiber and matrix result in the fatigue properties of natural fiber reinforced composites being different from synthetic fiber reinforced composites.

In terms of mechanical properties, flax is one of the strongest fibers in the natural fiber family. Flax fiber reinforced composites possess good vibration absorption capacity and the load required to initiate damage in flax fiber reinforced composites is significantly higher than in jute fiber reinforced composites [8]. Flax fiber can even be considered to be more fatigue resistant than glass fiber because the strength degradation rate of flax fiber composites are lower than the glass fiber reinforced composites [9].

In order to use flax fiber reinforced polymer matrix composites as a high performance structural materials, knowledge about the fatigue limit of those materials is very crucial. Traditionally to define fatigue limit, fatigue test have been conducted at lower loading frequency to minimize the temperature development within the sample due to repetitive loading. To use flax fiber reinforced composites under high frequency vibrational loading, it is also important to know the effect of loading frequency on the fatigue limit of flax fiber reinforced composites. However,

at higher loading frequency materials may experience significant thermal degradation due to high temperature development within the sample. Therefore, it is also necessary to separate the thermal damage and damage due to cyclic loading at higher loading frequency in order to obtain a complete idea about the effect of loading frequency on fatigue life.

1.2. Objectives

The objectives of this study are:

1. Define the fatigue limit of unidirectional flax fiber reinforced polymer matrix composites through high cycle fatigue strength (HCFS).

2. Understand the effect of loading frequency on the HCFS of unidirectional flax fiber reinforced composites.

3. Define the thermal and damage creation energies generated during cyclic loading of flax fiber reinforced composites in order to separate their effect on fatigue life or fatigue limit.

2. DETERMINATION OF HIGH CYCLE FATIGUE STRENGTH OF UNIDIRECTIONAL FLAX FIBER REINFORCED COMPOSITES

2.1. Introduction

Most engineering materials have a safe limit of fatigue stress or endurance limit below which failure will not occur, but fiber reinforced polymer matrix composites do not exhibit such fatigue limits. Instead, gradual damage accumulation takes place during the entire life of a composite and eventually leads to failure, even at low applied stresses [10]. Generally, for composite materials, the fatigue limit is defined by using high cycle fatigue strength (HCFS), which is defined as the stress level at which material can survive up-to 10^6 to 10^8 cycles before failure [11].

Due to the inherent nature of fatigue failure, fatigue life can vary significantly from sample to sample. Zhao [12] experimentally defined the effect of loading ratio on fatigue life of basalt fiber reinforced composites and reported a significant variation in fatigue life from sample to sample. In addition, fatigue life can vary even more due to the heterogeneous properties of plant based fibers, imperfect alignment of fibers, and substantial non-uniform void content due to processing methods [13]. Moreover, performing a fatigue test for 10^6 to 10^8 cycles to define HCFS is very time consuming. Therefore, it is essential to have a model that can predict the fatigue limit (through HCFS) of composite materials within a short time without performing a full test. Stiffness degradation, thermographic, and energy dissipation-based models are currently used for predicting the fatigue limit and fatigue life of both metals and composite materials.

Unlike conventional/synthetic fiber reinforced composite, a stiffness degradation-based model is not suitable to predict fatigue life of natural fiber reinforced composites. While glass/conventional fiber reinforced composites show a significant decrease in stiffness before

failure due to fatigue loading, natural fiber reinforced composites show very little change in stiffness before failure due to fatigue loading [14]. Because of the reorientation of elementary microfibrils, natural fiber reinforced composites exhibit around a 5% increase in initial stiffness during initial fatigue cycles, and this increased stiffness remains unchanged until the failure [15] [16].

Temperature-based models that predict fatigue life have been presented in literature. Ristiano [17] proposed a temperature-based model to predict the fatigue life of steel samples. Fatigue samples become heated substantially due to mechanical work on the sample by the fluctuating load and the temperature becomes stabilized after a few initial fatigue cycles. The stabilized temperature was used to define a parameter ($\phi \approx \Delta T \times N_f$) that is fixed at all stress levels, which can predict fatigue life at different stress levels for steel [18]. A slightly modified parameter ($\phi = \Delta T \times \log(N_f)$) was proposed by Montesano [19] for carbon fiber reinforced composites. Moreover, a more general parameter ($\phi = \Delta T \times N_f^{\frac{1}{\alpha}}$) was proposed by Huang [20].

Thermographic (based on stabilized temperature) and energy dissipation per fatigue cycle based approaches to predict fatigue limit (HCFS) are very accurate and timesaving [21, 22]. Both thermographic and energy dissipation per cycle based approaches were used to define the fatigue limit of carbon fiber reinforced composites by Montesano [19]. Jeannin [11] used an experimental approach to define HCFS of flax-epoxy reinforced composites, but the thermographic approach was also successfully used to define the fatigue limit of flax fiber reinforced composites [10]. Furthermore, specific damping capacity (energy loss) was used to determine the critical load for damage initiation in the cases of jute and flax fiber reinforced composites by Gassan [8]. However, an approach whereby energy dissipation per fatigue cycle is calculated has so far not been used to define the HCFS of flax fiber reinforced composites.

The overall goal of this study is to define the long term reliability of the flax fiber reinforced polymer matrix composites through fatigue testing. In this current study, a mathematical model is proposed to predict the fatigue life of flax fiber reinforced composites, and both thermographic and energy dissipation per cycle based approaches are used to define the fatigue limit through HCFS of unidirectional flax fiber reinforced composites.

2.2. Materials and methods

To define the long term reliability of flax fiber reinforced composite, material was manufactured using unidirectional flax fiber and epoxy resin. Unidirectional (UD) flax fiber (non-crimp, 105 tex) was purchased from BComp amplitex and fabric that was made from UD flax fiber (weft thread = 1/cm) has a weight of 300 gsm (Figure 1 (a)). The infusion epoxy resin (pro-set, INF-114) with an amide hardener having a medium cure speed (INF-211) was used as a matrix material (Figure 1 (b)). The amide hardener was used to crosslink the epoxy resin. The mixed resin have the viscosity of 296 cP, and density of 9.5 lb/gal at 22˚C and the cured resin have glass transition temperature (T_g) of 85℃.

(a) (b)

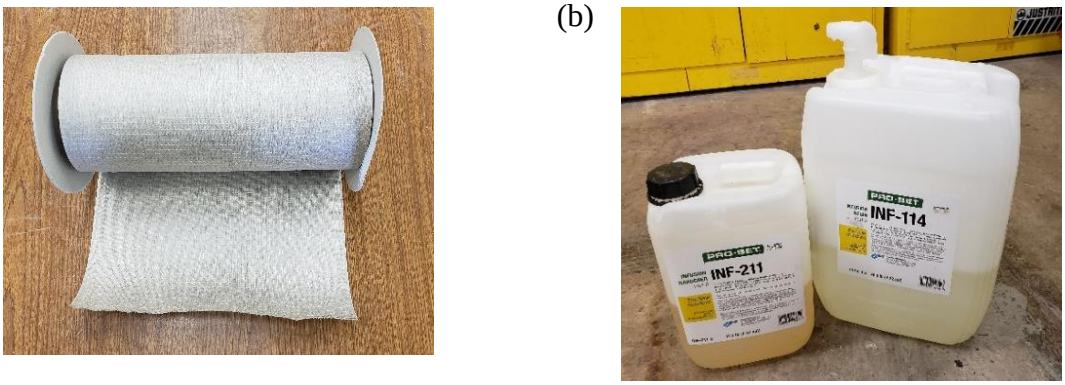

Figure 1: (a) Unidirectional flax fiber (b) Epoxy resin (proset) with amide hardener.

As shown in Figure 2, to produce thermoset composites using those fiber and resin, The VARTM (vacuum assisted resin transfer molding) process was used. Twelve layers of unidirectional flax fiber fabric were stacked on the table. A distribution medium was placed on the top of the stacked fiber to ensure good infusion of resin into the fiber. Vacuum bagging was inserted on those stacked fiber to make an air tight chamber. A pump was used to create a vaccum in the interior and then resin was infused into the stacked fiber by using vacuum pressure. To ensure complete curing, post cure was conducted for 3 days at room temperature and for 8 hours at 80 °C. The fiber volume fraction of those unidirectional flax fiber reinforced composites was about 50%.

Figure 2: Vacuum assisted resin transfer molding to make composite panel $[0]_{12}$.

Boards of flax fiber reinforced composite produced by VARTM were cut down into standard size using a ceramic tile saw in order to make samples for mechanical testing. Samples were cut according to the ASTM 3039 [23] standard for polymer matrix composites and a glass fiber tab was added to the sample in order to ensure better load transfer during testing (Figure 3). The length of each sample was 10 inches with a width of 1 inch. Each tab was 2.25 inches long. The edge of the tabbing material was cut down with a chamfer of 45° to avoid stress concentration at tip of the tab materials.

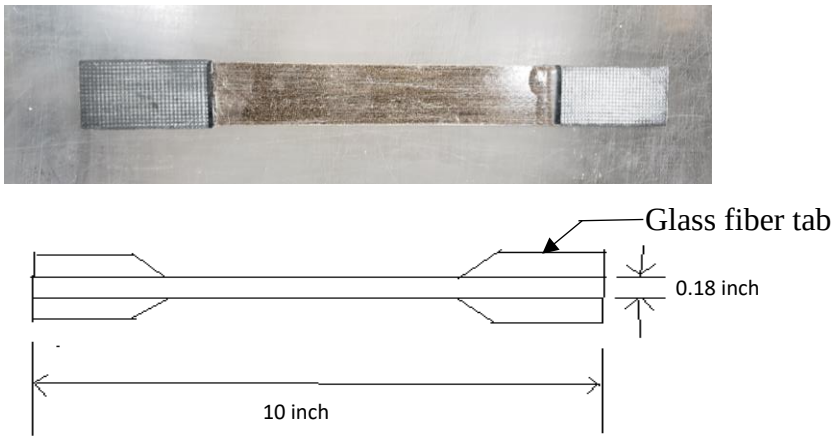

Figure 3: Test sample

A Servo hydraulic MTS machine with 250 kN load cell was used to perform all tensile and fatigue testing. Although the maximum applied force on the sample during testing was below 35 kN, but the machine has the load application error of less than 250 N. All tensile tests were done according to ASTM D3039 [23] standard and all fatigue tests were done according to ASTM D3479 [24] standard.

In order to evaluate the fatigue behavior of a composite, the sample was first tested monotonically to obtain information about its ultimate tensile strength (UTS). The tension-tension fatigue test was accomplished in load control mode at different percentage load (30, 35, 40, 45, 50, 55, 60, and 70%) of UTS, and the load variation during those fatigue test was sinusoidal (Figure 4). The maximum applied load of that sinusoidal load variation was the different percentage load of UTS and the minimum applied load of that sinusoidal load variation was 10% of maximum load. The minimum applied load also can be defined using a loading ratio. This loading ratio is defined as the ratio of maximum load to minimum load during fatigue testing (Equation (1)). In this current study, all test were performed with loading ratio, R = 0.1.

$$\text{Loading ratio, } R = \frac{\sigma_{min}}{\sigma_{max}} = \frac{F_{min}}{F_{max}} \quad (1)$$

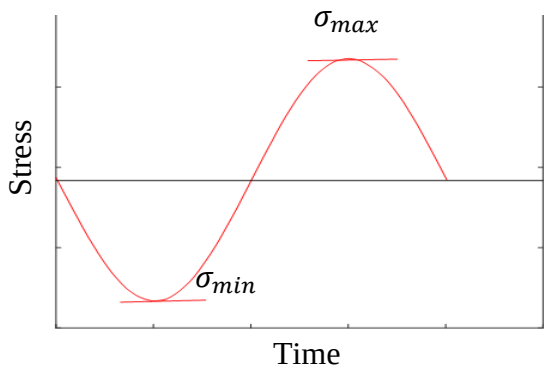

Figure 4: Sinusoidal load variation during cyclic loading

One complete fatigue cycle consisted of one loading and one unloading portion. The number of fatigue cycles completed per second is defined as loading frequency (f). All fatigue tests were performed at 5 Hz loading frequency. At higher loading frequencies, for different materials and different stress levels the machine needed to be tuned using proportional integral (PI) tuning. The PI tuning parameter was fixed in a way to ensure error in the applied load was below ±5%.

2.3. Results and discussion

2.3.1. Tensile tests

In order to determine the ultimate tensile strength (UTS) of the material, tensile tests were conducted using the MTS load frame in displacement control mode with a crosshead displacement of 0.05 inch/min. Figure 5 exhibits the stress-strain diagram for the monotonic tensile test of samples and the UTS of the flax fiber reinforced composites was around 300 MPa. The stress–strain curve of plant based fiber reinforced polymer matrix composites exhibits non-linear behavior, which is also clear from Figure 5. The tensile test curve also shows two linear regions with a yield point at their inflection. The first region represents the elastic strain and the second region is viscoelastoplastic with irreversible strain [25, 26]. A decrease of stiffness was found at

the second region of the tensile test curve probably due to the rotation and separation of some single fiber from the fiber bundles [27]. This decrease represents fiber dominated behavior and the rate of decrease (strain softening) depends on the volume fraction of fibers [6]. Synthetic fiber reinforced composites or pure resins do not exhibit such non-linearity during their tensile tests [25]. Furthermore, the ultimate tensile strength disperses little from sample to sample, which indicates the reproducibility of the materials.

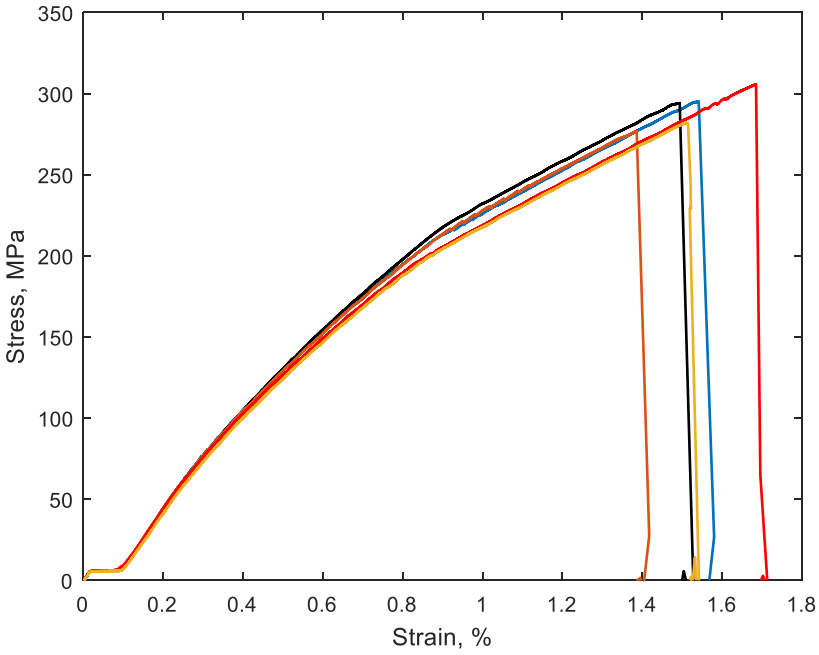

Figure 5: Tensile tests of flax fiber reinforced epoxy composites $[0]_{12}$.

2.3.2. Fatigue tests

Fatigue tests were conducted at different percentages of ultimate tensile strength (UTS) on the material with a loading frequency of 5 Hz. Figure 6 presents the comparison of fatigue life of flax fiber reinforced composites at stress levels of 60, 70, and 80% of UTS. Such a comparison is known as S-N diagram. Ten samples were tested under fatigue loading at each stress level. As expected, fatigue life decreases with increasing applied stress. As mentioned before, due to the nature of the fatigue tests, the heterogeneity of the plant fibers, and the manufacturing process,

data of fatigue life was very scattered. Figure 7 shows the picture of some samples tested under cyclic loading. Failure of the sample generally occur very near to the grip. It is very challenging to avoid failure very near to the grip in case of unidirectional composites. Figure 8 exhibited the scanning electron microscopy (SEM) images of the sample tested under tensile and fatigue loading. It is vivid from the Figure 8 that main failure mode of those samples are fiber pull-out. Sample failed under fatigue loading shows some rotation among the fiber bundle whereas sample failed under tensile test does not shows such rotation. Moreover, in real life applications, materials are always used at lower stress levels to obtain a prolonged life. One single fatigue test at a lower stress level would take couple of days to finish at a loading frequency of 5 Hz.

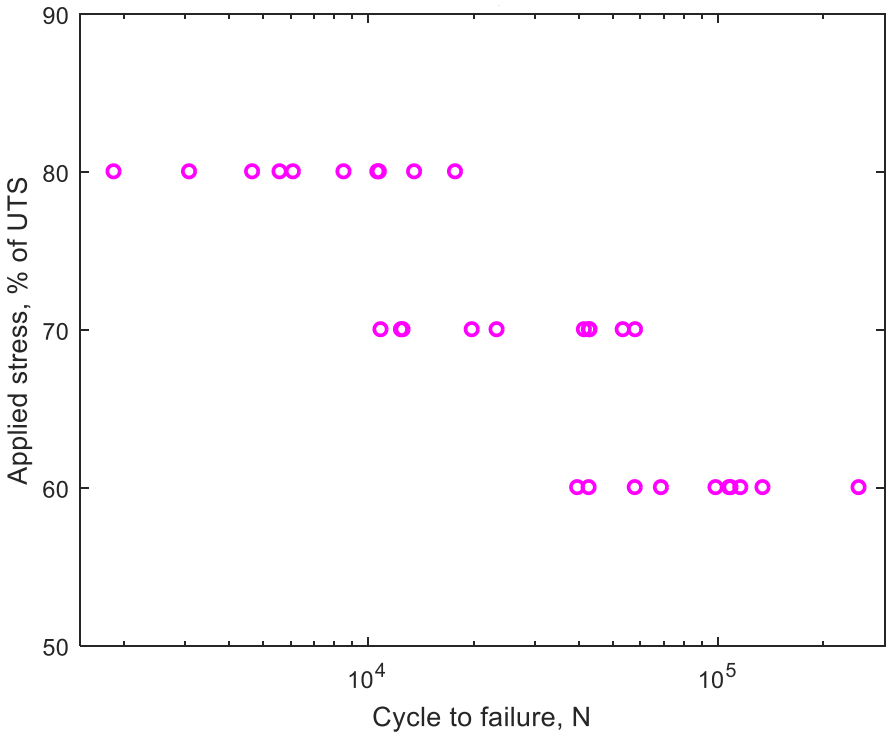

Figure 6: S-N diagram (loading frequency = 5 Hz).

Figure 7: Fracture samples after fatigue testing.

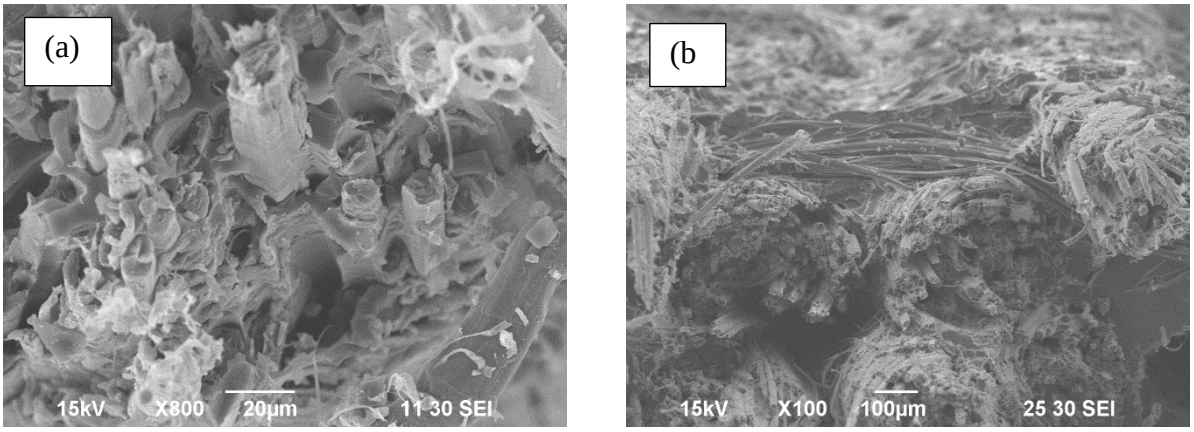

Figure 8: SEM images of fracture surface (a) Tensile test sample (b) Fatigue test sample, 80% UTS, 5 Hz

2.3.3. Self-heating of samples

Like metal and synthetic fiber reinforced composites, it was observed that, the temperature of the sample of unidirectional flax fiber reinforced composite increased significantly because of the mechanical work on the sample during cyclic loading. A portion of this mechanical work

applied to the sample during cyclic loading converted into heat energy, which causes the sample to self-heat. Increase of the sample temperature occurs due to the viscoelastic behavior of both natural fiber and resin and the interfacial shear/friction between the fiber and matrix [19, 28, 29]. Most synthetic fibers are fairly elastic in nature but the natural fibers exhibit viscoelasticity like polymeric resins. Interfacial friction at the interface of the fiber and the matrix depends on the roughness at their interface, the mismatch of their Poisson ratios, and the difference in their thermal expansions [30]. This self-heating temperature of the sample is directly related to the stress and damage developed in the material due to cyclic loading [5, 31]. A thermal IR camera (FLIR C2, range: -10℃ to 150℃, sensitivity: ±2℃) was used to capture thermal images in order to record the temperature reading of the sample during fatigue testing. Figure 9 shows the experimental set-up of the IR camera to capture thermal images and store it into a data logger. The surface temperature of the sample was not completely uniform all over sample, therefore the temperature at the center of the sample was recorded. Figure 10 exhibits the temperature increase pattern of the samples with respect to the fatigue cycles for different percentages of applied stress at a loading frequency of 5 Hz. During the initial fatigue cycles, the temperature of the sample increases rapidly and after a few initial fatigue cycles the temperature of the sample become stabilized. At higher percentages of applied stress, the temperature increase pattern of the sample presents a peak and then drops down to a stabilized temperature. These temperature peaks imply that, the materials have very high damage during the initial fatigue cycles compared to the stable damage during the stabilized surface temperature of the sample. However, the self-heating temperatures of those samples are much lower than the glass transition temperature of the used matrix materials (epoxy, 85℃).

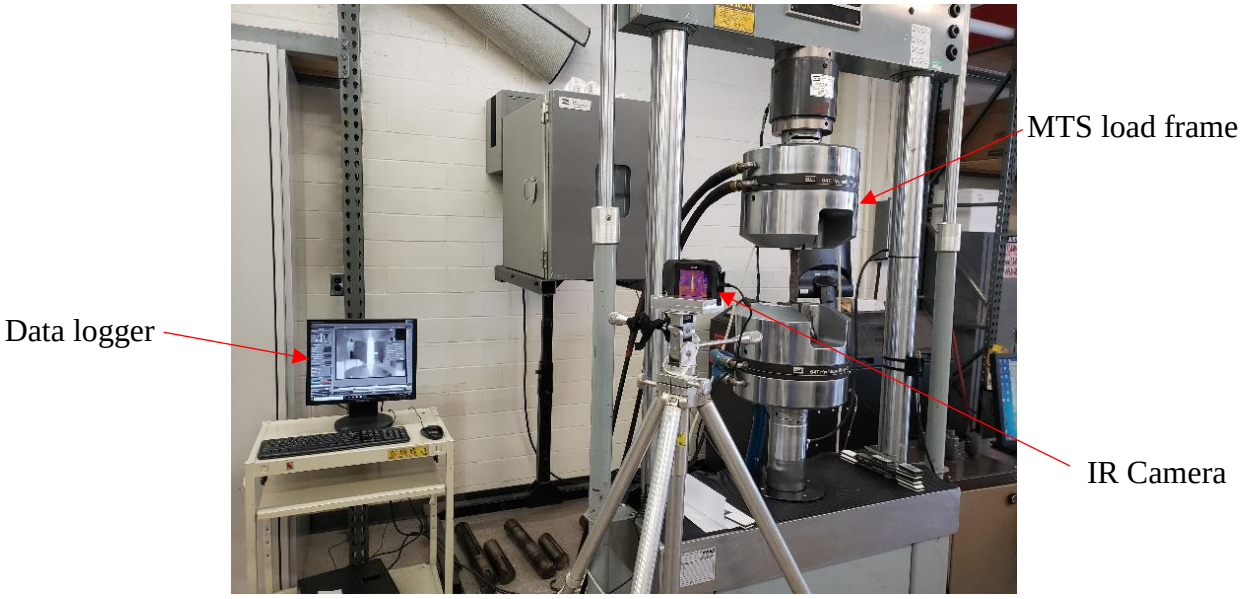

Figure 9: Temperature measurement of the sample during cyclic loading using IR camera.

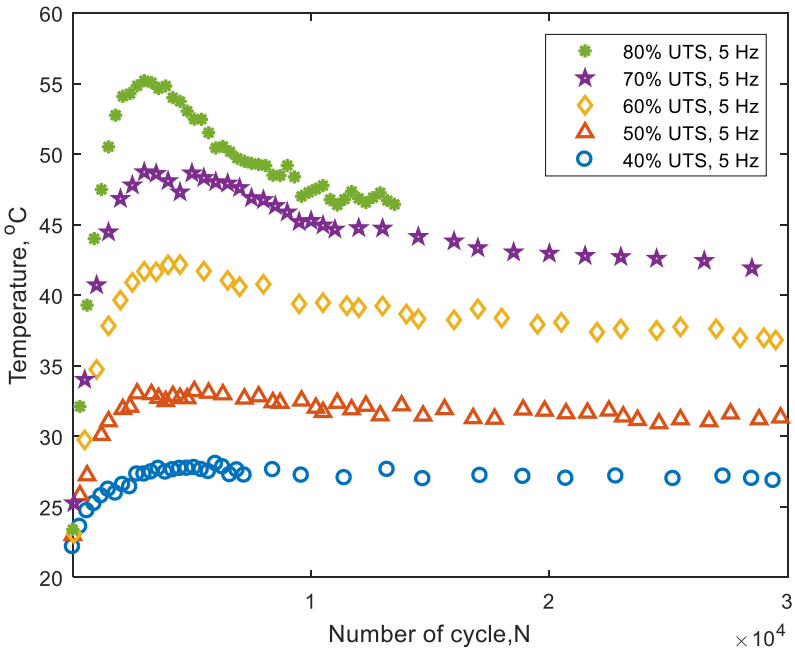

Figure 10: Temperature distribution of the fatigue sample at different percentages of applied stress (f = 5 Hz).

One portion of the heat energy generated during the cyclic loading transfers to the surroundings through conduction, convection or radiation (mostly convection, due to low thermal

conductivity of composites) and the other portion of the heat energy is stored in the sample, which causes the temperature of the sample to increase. The distribution of the heat energy generated due to the cyclic loading can be shown by Equation (2).

$$H_{generation} = H_{cv+cd+ir} + \rho c \frac{dT}{dt} \quad (2)$$

Where $H_{genaration}$ is the heat energy generated due to the cyclic loading, $H_{cv+cd+ir}$ is the heat energy conducted, convected or radiated to the surrounding, and $\rho c \frac{dT}{dt}$ is the heat energy stored in the sample to cause temperature change.

In order maintain a stabilized temperature all heat generated due to cyclic loading has to transfer to the surroundings by means of conduction, convection and radiation. No energy stored in the sample when the temperature is stabilized$\left(\rho c \frac{dT}{dt} = 0\right)$. Heat energy balance equation during temperature stabilization is given by Equation (3)

$$H_{generation} = H_{cv+cd+ir} \quad (3)$$

At higher percentages of applied stress, to create higher strain in the material, the material has to overcome high interfacial sliding resistance [30], therefore $H_{genaration}$ has higher value at the beginning of the cycling loading. Hence, during some initial fatigue cycles more energy will be stored into the sample, which will make the sample heated significantly. After a certain number of cycles, $H_{genaration}$ starts to decrease due to decrease of the interfacial sliding resistance, and come to a stable value to make the temperature stabilized. Therefore, a temperature peak was observed in the temperature distribution in Figure 10 at higher percentages of applied stresses. Such temperature peak was not observed at the lower percentages of applied stress. At lower percentages of applied stress, $H_{genaration}$ has lower value at the beginning due to lower strain created in the materials. Moreover, cycle/time required to attain stabilized temperature during

cyclic loading is more at higher percentages of applied stress as compared to lower percentages of applied stress.

Although the fatigue life fluctuates significantly from sample to sample, for a fixed applied stress, the stabilized temperature during the fatigue test is almost same for every sample. Therefore, the stabilized temperature is a unique characteristics of a fatigue test. Hence, the stabilized temperature based model to predict fatigue life is more convenient and reliable.

2.3.4. Mathematical model

As proposed by Huang [20], for different percentages of applied stress $\Delta T \times N_f^{\frac{1}{a}}$ always holds a constant value (Equation (4)).

$$\Delta T \times N_f^{\frac{1}{a}} = constant \tag{4}$$

Where, ΔT is the difference between room temperature and stabilized surface temperature of the sample during cyclic loading, N_f is the cycle required to material fail or fatigue life, and 'a' is a constant. Value of 'a' can be determined using regression analysis of experimental data.

Table 1 shows the fatigue life (N_f) and temperature increase (ΔT) of the sample at 60, 70, and 80% load of ultimate tensile strength (UTS). Equation (5) was obtained from Equation (4) by linear regression with the experimental data from Table 1.

$$\Delta T \times N_f^{\frac{1}{6.2556}} = 100.2972 \tag{5}$$

Table 1 also provides the value of $\Delta T \times N_f^{\frac{1}{a}}$ for different experimental results, which is almost close to the value that was obtained from the linear regression shown in Equation (5). The beauty of Equation (5) is that it can predict fatigue life of sample from the data of temperature increases (difference between stabilized temperature and room temperature,ΔT) of the sample

during fatigue testing. As temperature become stabilized after limited number of cycle, it requires run fatigue test for a short period of time to predict fatigue life using Equation (5). Using Equation (5), it is possible to predict the fatigue life of sample without performing a full test as shown in Table 2.

Table 1: Experimental Data for Fatigue Test at Different Level of Applied Stress.

% of UTS	ΔT (°C)	N_f	$\Delta T \times N_f^{\frac{1}{a}}$
60	15	108161	95.68
		134827	99.11
		116516	99.30
		69072	89.06
		98964	94.33
		109239	95.83
		42919	82.53
		253797	109.65
		58145	86.64
		39803	81.54
70	20	41616	109.50
		42991	110.07
		58262	115.56
		43190	110.16
		53723	114.07
		10906	88.40
		19880	97.31
		12476	90.32
		23417	99.89
		12610	90.48
80	26	13605	118.92
		8548	110.53
		10681	114.54
		10789	114.72
		3092	93.95
		4683	100.39
		1881	86.77
		17810	124.299
		5166	101.98
		6125	104.80

Table 2, shows the predicted value of fatigue life from the experimental data of temperature increase (ΔT) during cyclic loading. As mentioned before, stress level at which material can survive up to 10^6 to 10^8 cycle is called high cycle fatigue strength (HCFS), Therefore it is clear from Table 2 that, HCFS of flax fiber reinforced composite will be between 40 to 50% load of UTS.

Table 2: Prediction of Fatigue Life from the Data of Stabilized Temperature during Cycling Loading.

% of UTS	ΔT (°C)	N_f(cycles)
50	9.5	2.52×10^6
45	5.5	7.72×10^7
40	4.5	2.71×10^8
35	2.5	1.07×10^{10}

2.3.5. Thermographic approach

Stabilized temperature at different percentage of applied stress during fatigue testing of unidirectional flax fiber reinforced composites were compared in Figure 11 and it shows a bilinear behavior with an inflection point. Stress level at which inflection occurs represents high cycle fatigue strength (HCFS). From Figure 11, it is clear that, unidirectional flax fiber reinforced composites have HCFS of around 45% of UTS which supports the results of mathematical model discussed in previous section. This means, for nearly 45% load of ultimate tensile strength material can survive up-to 10^6 to 10^8 cycle during fatigue testing with loading ratio, R = 0.1 and loading frequency, f = 5 Hz.

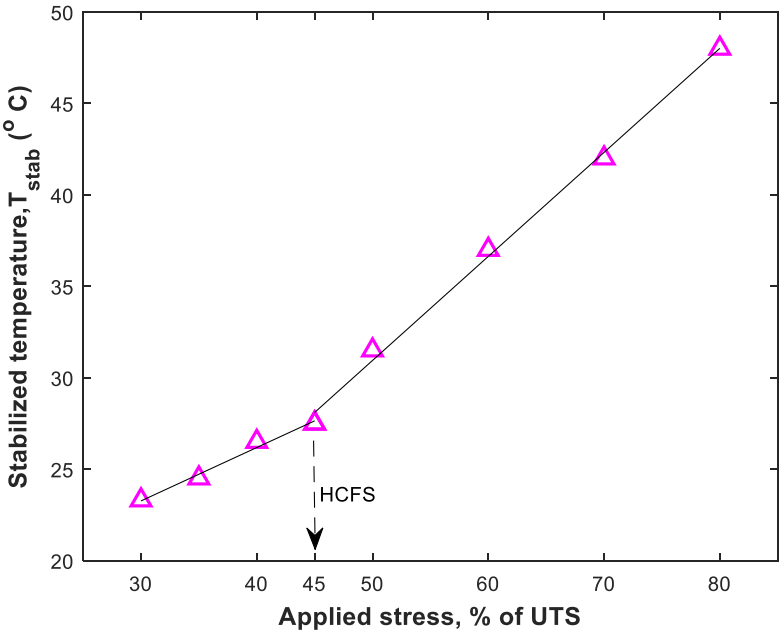

Figure 11: Thermographic approach to define the HCFS of unidirectional flax fiber reinforced composites.

2.3.6. Dissipated energy per cycle based approach

As mentioned earlier, the energy dissipation per cycle based approach was used to predict the HCFS of synthetic fiber reinforced composites, but has not been demonstrated for flax fiber reinforced composites. In this current study, the energy dissipation per cycle based approach is also used to define the HCFS of unidirectional flax fiber reinforced composites. Figure 12 exhibits the load–displacement diagram of a single fatigue cycle (i.e. hysteresis curve). The upper portion of the hysteresis curve represents the loading cycle and the lower portion represents the unloading cycle. During the loading cycle, some amount of mechanical work was done on the sample, and during the unloading cycle a portion of this mechanical energy was released. The area enclosed by the loading and unloading cycle represents the energy dissipated for a single fatigue cycle [19]. In order to record the data of loads and displacements during fatigue testing, the data acquisition frequency was set as to obtain 102 data points for a single fatigue cycle.

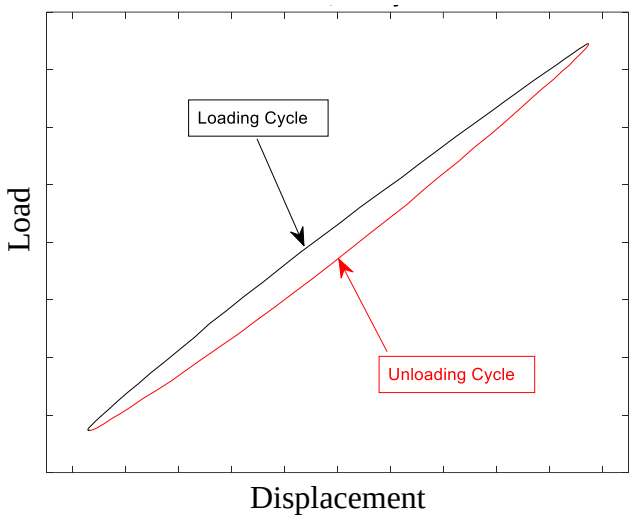

Figure 12: Load-displacement diagram for a single fatigue cycle (i.e. hysteresis loop).

Figure 13 depicts the method of determining the dissipated energy per cycle during cyclic loading. The area under the loading cycle represents the energy absorbed by the sample (Figure 13(a)), and the area under the unloading cycle (Figure 13 (b)) represents the energy released by the sample (Figure 13 (b)). The difference of those two energies represents the total dissipated energy per cycle (Figure 13 (c)). The total dissipated energy per cycle is consumed in two ways; as shown in Equation (6), one portion of energy is converted to heat energy $\left(H_{generation}\right)$and the other portion creates internal micro-mechanical damage $\left(E_{damage}\right)$ in the sample [32-34]. Internal micro-mechanical damage includes micro-crack initiation and the slow propagation of these cracks to make the material fail.

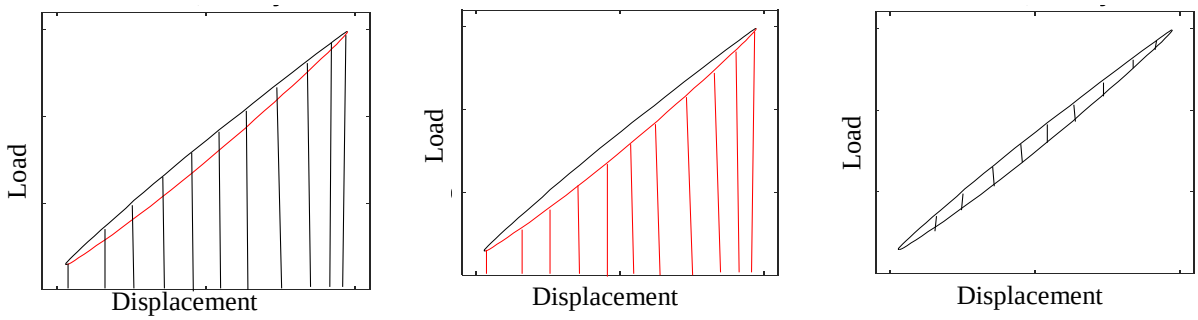

(a) (b) (c)

Figure 13: Method of determining dissipated energy per fatigue cycle. (a) Area under the loading cycle/ energy absorbed by the sample during loading cycle, (b) Area under the unloading cycle/ energy released by the sample during unloading cycle, (c) Total dissipated energy during a single fatigue cycle.

$$\oint(\sigma\, d\varepsilon).\ f = H_{generation} + E_{damage} \tag{6}$$

Figure 14 provides the distribution of dissipated energy per cycle over the fatigue life of the sample at different percentages of applied stress (% UTS) for the loading frequency of 5 Hz. With the increase of the percentage of applied stress (% UTS), the dissipated energy per cycle also increases. For all percentages of applied stress, the dissipated energy per cycle was higher during the initial fatigue cycles. This occurs because high initial micro-damage was created over the entire composite sample during those initial fatigue cycles. Just like the temperature results, after a few initial cycles, the dissipated energy per cycle begins to decrease and become stabilized, which represents stable damage progression for the rest of the fatigue life. At higher percentages of applied stress, energy dissipation per cycle during the initial fatigue cycles is almost double than the stabilized dissipated energy per cycle. Hence, the initial damage is very high at higher percentages of stress level. At lower percentages of applied stress, the difference in energy dissipation per cycle during the initial and stabilized fatigue cycle is not as large. Moreover, the number of fatigue cycles required to reach the stable dissipated energy per cycle is less at lower

percentages of applied stress. Therefore, the initial fatigue damage is not as detrimental at lower percentages of applied stress.

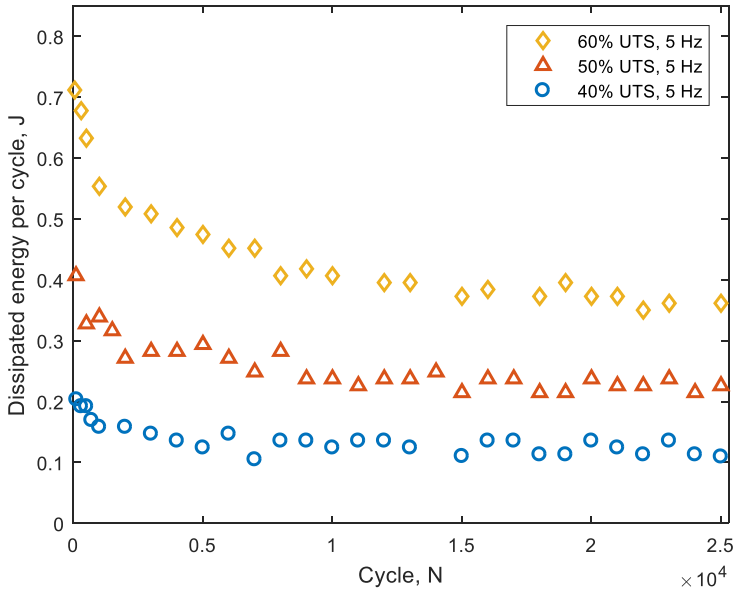

Figure 14: Distribution of dissipated energy per cycle during fatigue loading at different percentage of applied stress.

Figure 15 compares the dissipated energy per cycle (after stabilization) with the percentages of applied stress, which shows a bilinear behavior with an inflection point just like the stabilized temperature. The inflection point at 45% of UTS represents that the material has an HCFS of 45% UTS for a loading frequency of 5 Hz, which is very similar to the HCFS obtained from the mathematical model and stabilized temperature-based thermographic method. Micro-mechanical damages developed in the material at stress levels below the HCFS is very negligible. Below the HCFS, energy dissipation is mainly due to the internal friction between fiber and matrix. Micro-mechanical damage become significant at stress levels above the HCFS, which makes the material fail rapidly [35].

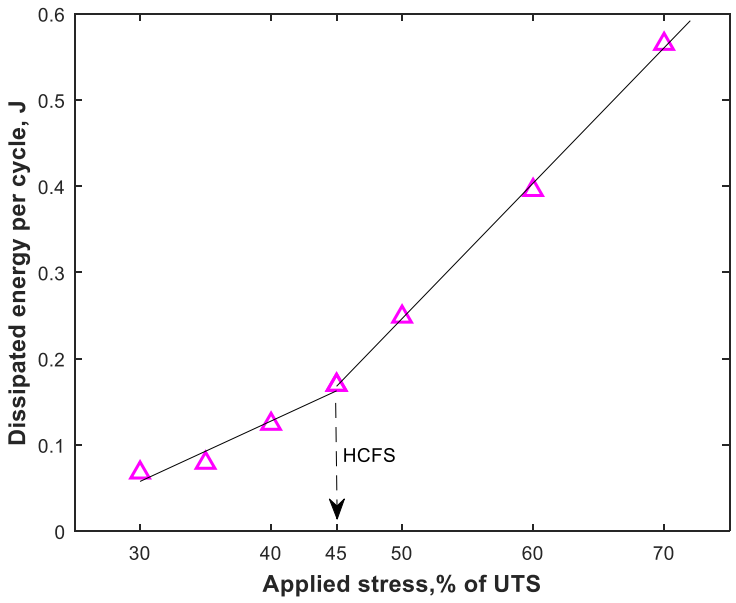

Figure 15: Dissipated energy per cycle based approach to define HCFS of unidirectional flax fiber reinforced composites.

Therefore, it is clear from the aforementioned results that the HCFS of the unidirectional flax fiber reinforced composites can be determined from both the stabilized temperature and the energy dissipated per cycle. Figure 16 provides the linear relationship between the stabilized temperature and the dissipated energy per cycle. Because of this linear relationship between the stabilized temperature and dissipated energy per cycle, both of them can be used to define the HCFS of flax fiber reinforced composites.

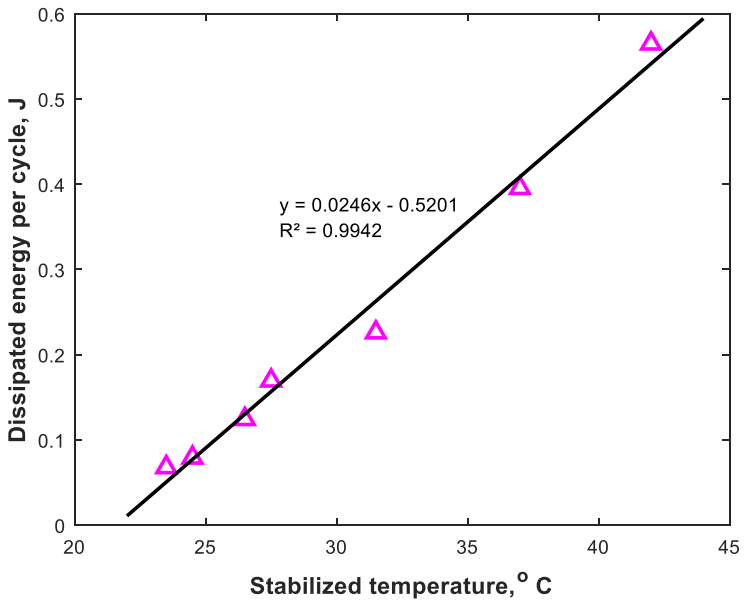

Figure 16: Linear relation between stabilized temperature and dissipated energy per cycle during fatigue loading at loading frequency, f = 5 Hz.

2.4. Conclusion

Mathematical model using experimental data, thermographic model using stabilized temperature during cyclic loading, and dissipated energy per cycle based approaches were used to define the HCFS of unidirectional flax fiber reinforced composites, which is about 45% load of UTS at a loading frequency of 5 Hz. Although one single fatigue test at lower percentages of applied stress would take couple of days to finish, the proposed mathematical model will be able to predict fatigue life at lower percentages of applied stress using the experimental data of fatigue life at higher percentages of applied stress. Moreover, HCFS of the unidirectional flax fiber reinforced composites was successfully determined using the thermographic and energy dissipation per cycle based approaches by running few fatigue test for a short time intervals. Both stabilized temperature (thermographic) and dissipated energy per cycle can be used to define the HCFS as they show linear behavior with one another. As HCFS would vary for different fiber orientations, hence a quick method for determining the HCFS of polymer matrix composites is

very essential. Changing the fiber architecture and conducting surface treatment of fibers to ensure better adherence between fiber and matrix can even increase the HCFS of flax fiber reinforced composite, which may create a path for flax fibers as a potential alternative of synthetic fibers in more performance demanding applications. The Triaxially braided carbon fiber reinforced polymer matrix composites have HCFS of 64% load of UTS [19]. It is expected, due to lower mechanical properties flax fiber reinforced composites might have lower HCFS than carbon fiber reinforced composites. However, unidirectional flax fiber reinforced composites shows reasonable HCFS (45% load of UTS), which can be improved further by laminating.

3. EFFECT OF LOADING FREQUENCY ON THE HIGH CYCLE FATIGUE STRENGTH OF FLAX FIBER REINFORCED POLYMER MATRIX COMPOSITES

3.1. Introduction

As fatigue is a frequently encountered loading condition on structural materials, the knowledge about the fatigue limit of a material is therefore crucial. Stress levels at which materials can survive more than 10^6 fatigue cycles is defined as the fatigue limit. In order to use a material for real-life high performance application with fluctuating loading, it is essential to have knowledge about the fatigue limit as that material should be used at a stress level under fatigue limit. To define the applicability of material under abrupt real life vibrational loading, it is important to know the effect of loading frequency on the fatigue life. Although loading frequency does not have significant effect on the fatigue life for metallic materials [36-38], composite materials exhibit some effect of loading frequency on the fatigue life [39-43]. Recently natural fiber reinforced composites have received significant attention due to their excellent mechanical properties along with renewability.

Flax is the strongest among natural fibers and have significant potential to substitute synthetic fiber due to its excellent mechanical and damping properties [8]. Moreover, flax fiber reinforced composites show excellent properties under cyclic/fatigue loading [14]. The fatigue limit of flax fiber reinforced composite was also reported in literature by performing full fatigue test [9-11, 44]. Furthermore, instead of doing full fatigue test, sample surface temperature based thermographic approach was successfully used to define fatigue limit of flax fiber reinforced composite materials [10]. Similar fatigue limit was exhibited both from full fatigue test and thermographic approach. Both thermographic and dissipated energy-per-cycle based approach was used to define fatigue limit of synthetic fiber reinforced composites (i.e. carbon fiber

reinforced composites) [19]. The thermographic and dissipated energy-per-cycle based approach are rapid and timesaving in determining fatigue limit accurately.

As the surface temperature of flax fiber reinforced polymer matrix composites increases significantly with increasing loading frequency during cyclic loading, under similar level of applied stresses the fatigue life of flax fiber reinforced composites therefore decreases with increasing loading frequency [11]. At higher loading frequency thermal degradation of the sample accumulates with fatigue damage [42]. Although some studies have exhibited the effect of loading frequency on fatigue life of flax fiber reinforced composites [11], very few studies have been attempted to find effect of loading frequency on the change of fatigue limit. Moreover, due to inherent variation in fatigue life between sample to sample [12], defining fatigue limit by conducting test until failure requires tremendous prolonged experimental efforts. Therefore, the overall goal of this study is to define the effect of loading frequency on the fatigue limit of flax fiber reinforced composites using thermographic and dissipated energy-per-cycle based approaches.

3.2. Materials and methods

As mentioned before in section 2.2, in order to make samples for fatigue testing, a panel (12 inch ×12 inch) of unidirectional flax fiber reinforced polymer matrix composites was manufactured using vacuum assisted resin transfer molding (VARTM). Fabric of non-crimp unidirectional flax fiber (105 tex, weft thread = 1/cm, weight =300 gsm) was purchased from BComp amplitex. The Infusion epoxy resin with amide hardener (mixed resin viscosity = 129 cP and density =9.5 lb/gal at 22 ˚C) was used as a matrix materials. Twelve layers of unidirectional flax fiber fabric was used to prepare the sample. Post curing was accomplished for 3 days at room

temperature and 8 hours at 80 °C. Volume fraction of produced board of unidirectional flax fiber was about 50%.

Test samples were prepared from produced boards using a ceramic cutter according to the ASTM 3039. Sample size was 10 in. long and 1 in. in width. Glass fiber tab of 2.25 in. long was inserted on each side of the sample to ensure better load transfer. All tensile and fatigue test was conducted using MTS 250 kN servo-hydraulic load frame. Tensile test was conducted to obtain information about the ultimate tensile strength (UTS) of the materials. Fatigue tests were conducted at different percentages of the ultimate tensile strength of the materials. Load variation during fatigue/cyclic loading was sinusoidal. Minimum applied stress during fatigue loading is 10% of the maximum applied stress which is defined as loading ratio, R = 0.1.

To define the effect of loading frequency on the fatigue limit through high cycle fatigue strength (HCFS) of flax fiber reinforced composites, fatigue test were conducted at different percentages of applied stress for the loading frequencies of 5, 7, 10, and 15 Hz. Due to the viscoelastic nature of natural fiber and resin, the sample become heated significantly during cyclic loading. An IR camera was used to capture the temperature distribution of the sample during cyclic loading. Both thermographic and energy dissipation per cycle based approach was used to define HCFS of flax fiber reinforced polymer matrix composites at those loading frequency. To determine the dissipated energy per fatigue cycle force and elongation data was captured during cyclic loading with a data acquisition frequency that endure around 102 data point per fatigue cycle.

3.3. Results

3.3.1. Temperature distribution

Figure 17 shows the temperature distribution of the sample during cycling loading for different percentages of applied stress at the loading frequencies of 5,7,10, and 15 Hz. In all cases,

initially the temperature of the sample increases rapidly and the temperature of the sample becomes stable after a certain number of cycles. At higher percentages of applied stress, temperature shows a peak and then becomes stable afterward. Figure 17 also depicts that, at higher percentages of applied stress, the sample takes more time or cycles to reach a stable temperature. This trend was observed at all loading frequencies. During temperature stabilization, sample temperature shows a small oscillatory variation due to thermoelastic effect [5]. This thermoelastic effect / oscillatory temperature variation is very low at lower percentage of applied stresses but comparatively high at higher percentage of applied stresses.

Figure 18 shows the effect of loading frequency on the stabilized temperature during cyclic loading. For same percentage of applied stress, the sample becomes stable at significantly higher temperature at the higher loading frequency. This is may be attributed to the viscoelastic effect of the materials and high interlinear shear rate between fiber and matrix. Figure 18 also exhibits that, for same percentages of applied stress with increase of loading frequency, the sample needs more number of cycles to reach stabilized temperature. As heat transfer is a function of time, therefore at higher loading frequency material needs significantly more number of fatigue cycles to get stabilized temperature. At higher loading frequency the temperature peak was also observed at lower percentages of applied stress.

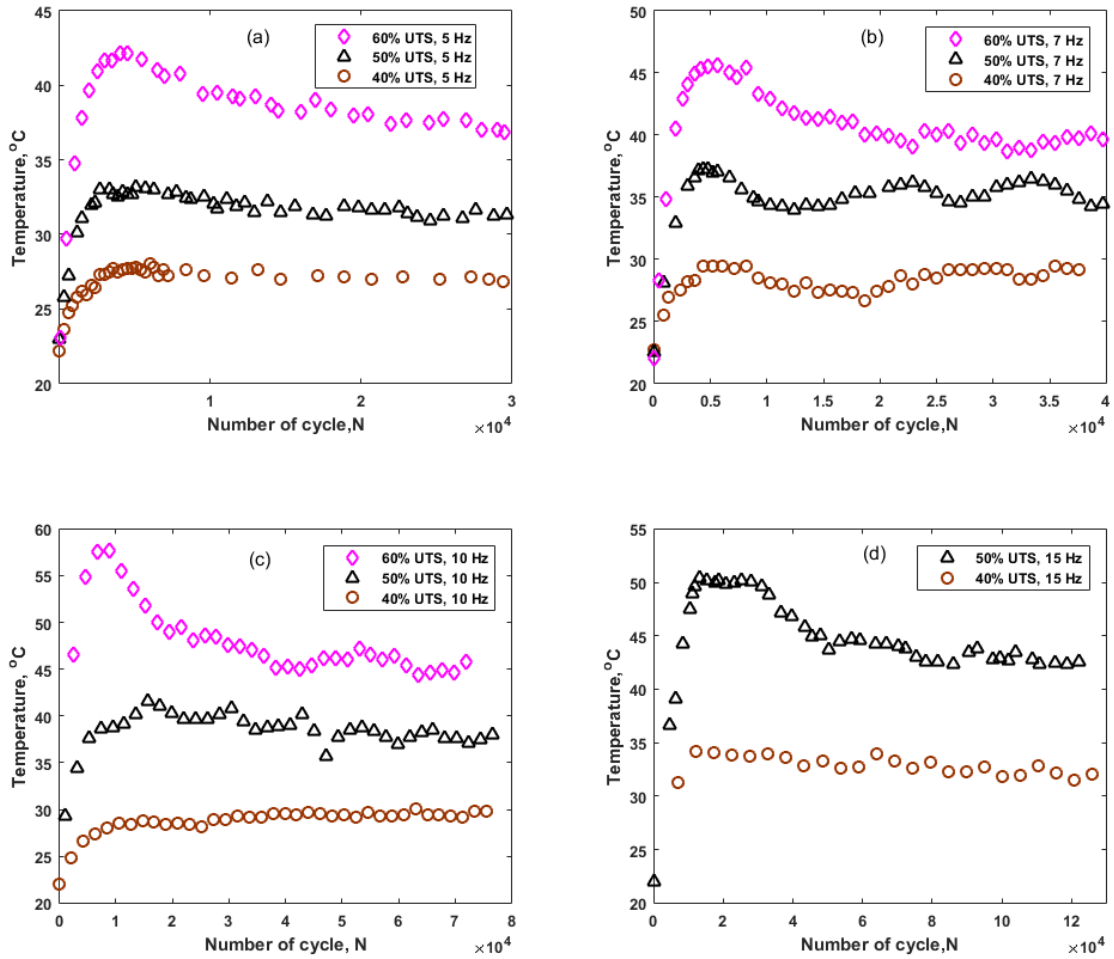

Figure 17: Temperature distribution of the sample tested under cyclic loading at 40, 50, and 60% load of UTS (a) at loading frequency = 5 Hz (b) at loading frequency = 7 Hz (c) at loading frequency = 10 Hz (d) at loading frequency= 15 Hz.

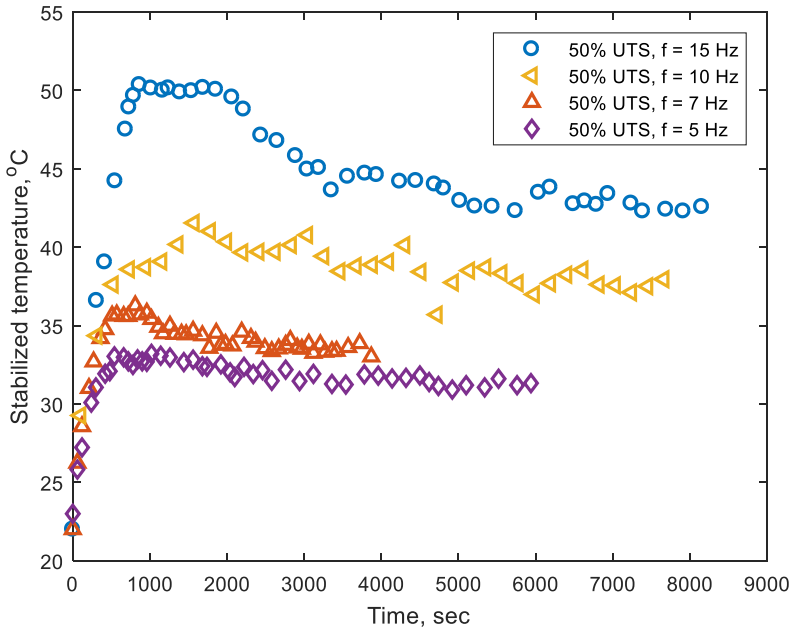

Figure 18: Temperature distribution of the sample tested under cyclic loading at 50% load of UTS for loading frequency of 5, 7, 10, and 15 Hz.

3.3.2. Energy distribution

As discussed in section 2.3.6, the force-displacement diagram for a single fatigue cycle consists of a loop having a loading and an unloading portion. These loops are called Hysteresis loop. The area under the hysteresis loop represents the dissipated energy during one single fatigue cycle [1]. Figure 19 shows the distribution of the dissipated energy per cycle during the cyclic loading at different percentages of applied stresses on the sample (40, 50, 60% load of UTS) for the loading frequencies of 5, 7, 10, and 15 Hz. For all cases, dissipated energy per cycle is higher during some few initial fatigue cycles and then reduce to a stable value with some small oscillatory fluctuations. As expected, dissipated energy per cycle increases with the increase of percentage of applied stress.

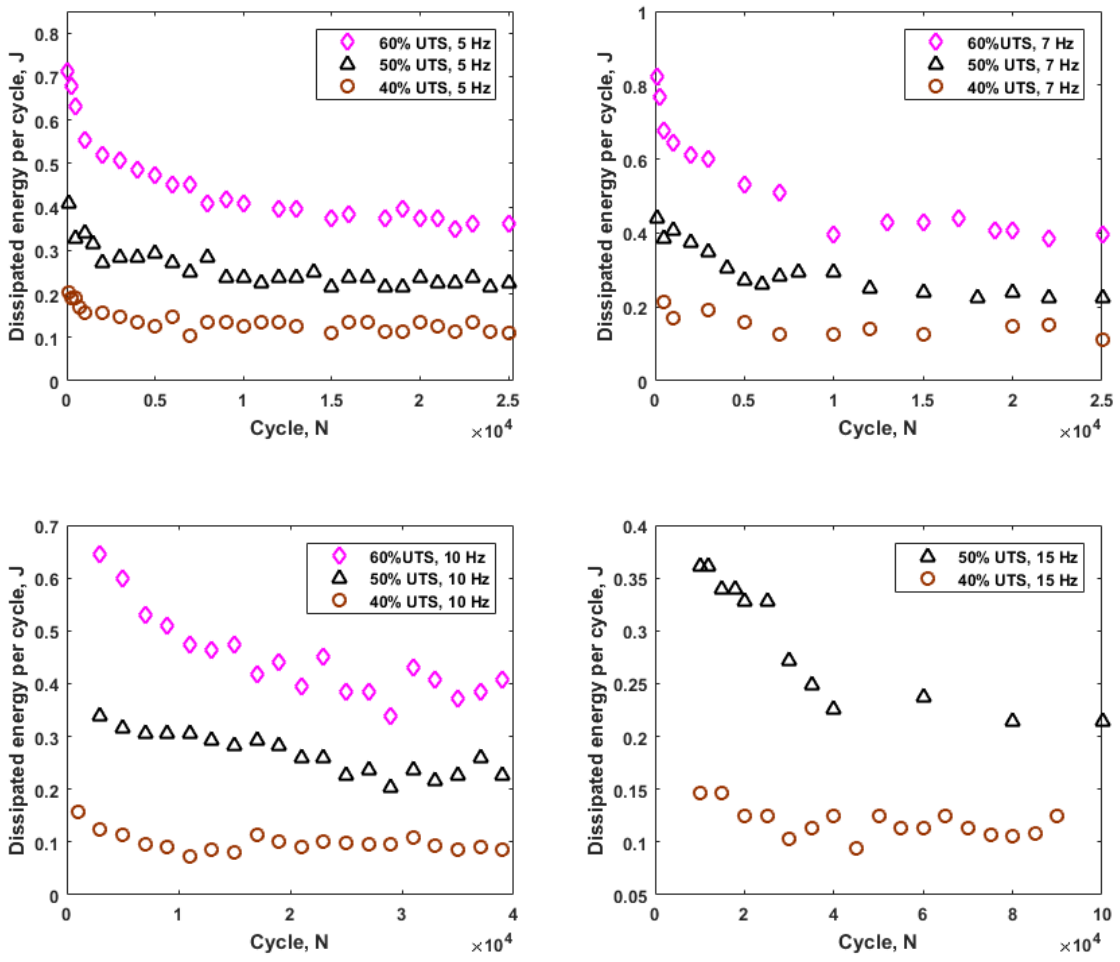

Figure 19: Distribution of dissipated energy per cycle at 40, 50, and 60% load of UTS (a) at loading frequency = 5 Hz, (b) at loading frequency = 7 Hz, (c) at loading frequency = 10 Hz, (d) at loading frequency = 15 Hz.

As shown in Figure 20, at the same percentage of applied stress (e.g. 50% load of UTS), the dissipated energy per cycle does not change significantly due to change of the loading frequency. For the 50% load of UTS, dissipated energy per cycle is almost same at 5, 7, 10, 15 Hz of loading frequencies. Although stabilized temperature increases significantly with increasing loading frequency, dissipated energy per cycle during cyclic loading vary little with loading frequency. A one-way ANOVA test was conducted on the data of dissipated energy per cycle at different loading frequencies. Table 3 shows five data points of stabilized dissipated energy per cycle at each loading frequency, which was used for one-way ANOVA test.

Table 4 shows the results of ANOVA test. As $p = 0.8406 \gg 0.05$, null hypothesis (means are equal) is accepted at the 5% level of significance that, there is no significant difference between the mean of total dissipated energy-per-cycle at different loading frequency.

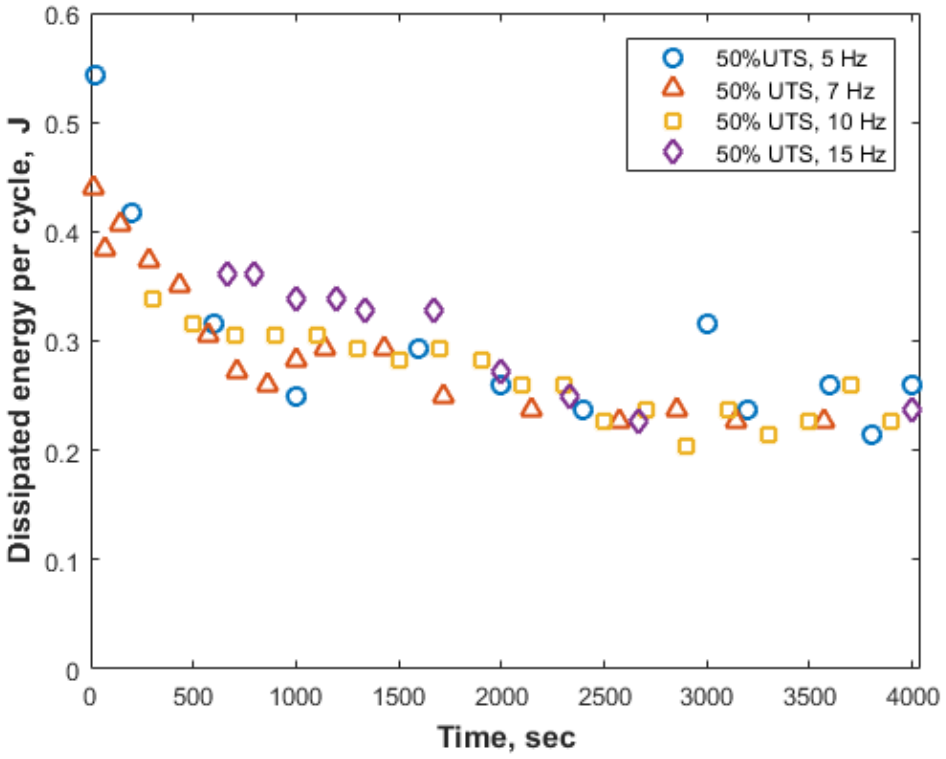

Figure 20: Distribution of dissipated energy per cycle at 50% load of UTS for loading frequency of 5, 7, 10, and 15 Hz.

Table 3: Dissipated Energy per Cycle (after damage stabilization) Data at Different Loading Frequency to Run One-way ANOVA Test.

	Group 1	Group 2	Group 3	Group 4
Frequency (Hz)	5	7	10	15
Dissipated energy per cycle(after stabilization), J	0.2260	0.2373	0.2373	0.2486
	0.2260	0.2260	0.2147	0.2260
	0.2373	0.2373	0.2260	0.2373
	0.2147	0.2260	0.2599	0.2147
	0.2260	0.2260	0.2260	0.2147

Table 4: Result of ANOVA Test on the Data of Dissipated Energy per Cycle at Different Loading Frequency from Table 3.

Source	Sum of Squares	Degree of freedom	Mean Square	F-ratio	P-value
Between groups	0.00013	3	0.00004	0.28	0.8406
Within groups	0.00245	16	0.00015		
Total	0.00258	19			

3.3.3. Thermographic approach for HCFS

Figure 21 compares the stabilized temperature during cyclic loading with different percentages of applied stress for the loading frequencies of 5, 7, 10, and 15 Hz. For all the loading frequencies stabilized temperature shows a bilinear behavior with an inflection point. Those inflection points represents HCFS. It is clear from the Figure 21 that HCFS is decreasing slowly with increasing loading frequency. Table 5 also shows the HCFS of unidirectional flax fiber reinforced composites using thermographic approach for loading frequencies of 5, 7, 10, and 15 Hz. As the loading frequency changes from 5 Hz to 15 Hz, HCFS changes from 45% load of UTS to 40% load of UTS. Furthermore, Table 6 shows the equation for the bilinear straight lines shown in Figure 21. The slope of those straight line is demonstrates an increasing trend with increasing loading frequency.

Table 5: HCFS of Unidirectional Flax Fiber Reinforced Composites at Different Loading Frequencies using Thermographic Approach.

Loading frequency, f	HCFS
5 Hz	45% UTS
7 Hz	42% UTS
10 Hz	41% UTS
15 Hz	40% UTS

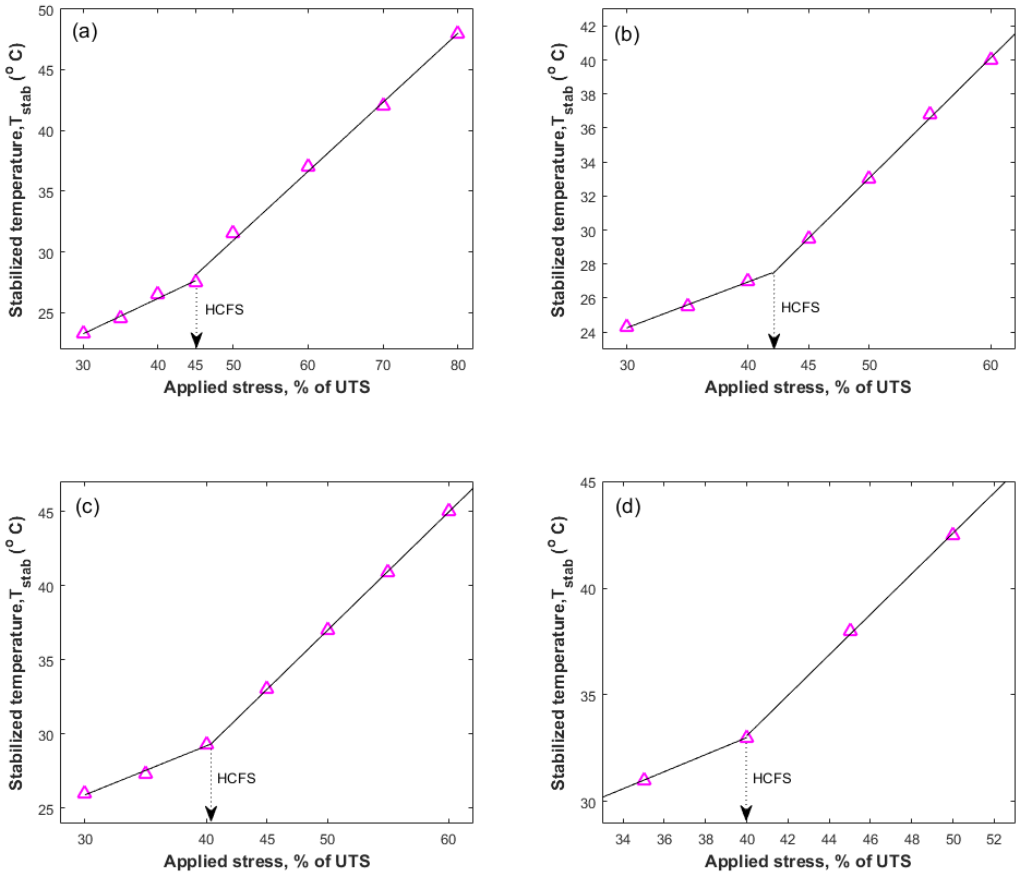

Figure 21: Thermographic approach to define fatigue limit (HCFS) at (a) loading frequency = 5 Hz, (b) loading frequency = 7Hz, (c) loading frequency = 10 Hz, (d) loading frequency =15 Hz.

Table 6: Equations for Bilinear Curve in Thermographic (Stabilized Sample Temperature Based) Approach to Determine HCFS.

Loading frequency	Equations
5 Hz	$y = 0.5689x + 2.1970;\ \ x > 45$ $y = 0.2920x + 14.5;\quad x < 45$
7 Hz	$y = 0.7060x - 2.24;\ \ x > 42$ $y = 0.270x + 16.15;\quad x < 42$
10 Hz	$y = 0.798x - 2.92;\quad x > 41$ $y = 0.33x + 15.98;\quad x < 41$
15 Hz	$y = 0.95x - 4.9167;\ \ x > 40$ $y = 0.40x + 17;\qquad x < 40$

Here, x represents the applied stress (% of UTS), and y represents the stabilized surface temperature of the sample.

3.3.4. Dissipated energy per cycle based approach for HCFS

Figure 22 compares the dissipated energy per cycle during cyclic loading with different percentages of applied stress for the loading frequencies of 5, 7, 10, and 15 Hz. Like stabilized temperature, those comparison also indicates a bilinear behavior with an inflection point. These inflection points also represents the HCFS. This dissipated energy based approach also provides similar results of HCFS like the stabilized temperature based approach. Table 7 shows the HCFS at different loading frequencies using dissipated energy per cycle based approach, which is almost similar of HCFS using thermographic approach shown in Table 5. Moreover, Table 8 exhibits the equations for those bilinear curves which may enable one to infer total dissipated energy per cycle at any arbitrary percentages of applied stress.

Table 7: HCFS of Unidirectional Flax Fiber Reinforced Composites at Different Loading Frequencies using Dissipated Energy per Cycle Based Approach.

Loading frequency	HCFS
5 Hz	45% UTS
7 Hz	43.3% UTS
10 Hz	40.5% UTS
15 Hz	40% UTS

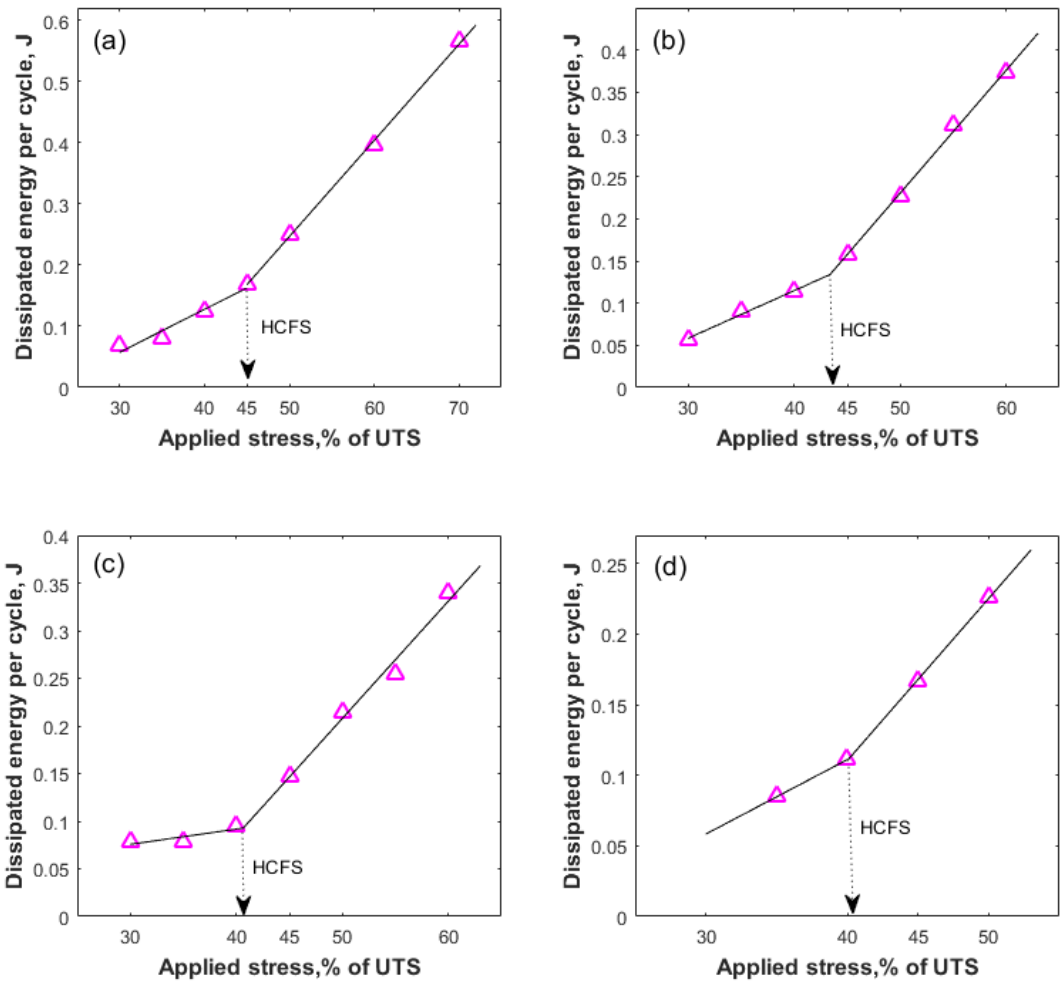

Figure 22: Dissipated energy per cycle (after stabilization) based approach to define fatigue limit (HCFS) at (a) loading frequency = 5 Hz, (b) loading frequency = 7Hz, (c) loading frequency = 10 Hz, (d) loading frequency =15 Hz.

Table 8: Equations for Bilinear Curve in Dissipated Energy per Cycle Based Approach to Determine HCFS.

Loading frequency	Equations
5 Hz	$y = 0.0157x - 0.5387;\ x > 45$ $y = 0.0070x - 0.1525;\quad x < 45$
7 Hz	$y = 0.0146x - 0.4983;\ x > 43.3$ $y = 0.0056x - 0.111;\quad x < 43.3$
10 Hz	$y = 0.0123x - 0.0479;\quad x > 40.5$ $y = 0.0016x + 0.0277;\quad x < 40.5$
15 Hz	$y = 0.0115x - 0.3491;\ x > 40$ $y = 0.0053x - 0.0998;\quad x < 40$

Here, x represents the applied stress (% of UTS), and y represents the total dissipated energy per fatigue cycle of the sample.

3.3.5. Linear relation between temperature and dissipated energy

Figure 23 exhibits the linear relationship between stabilized temperature and dissipated energy per cycle for the loading frequencies of 5, 7, 10, and 15 Hz. Because of this linear relation between stabilized temperature and dissipated energy per cycle during cyclic loading, HCFS can be determined by using either of them.

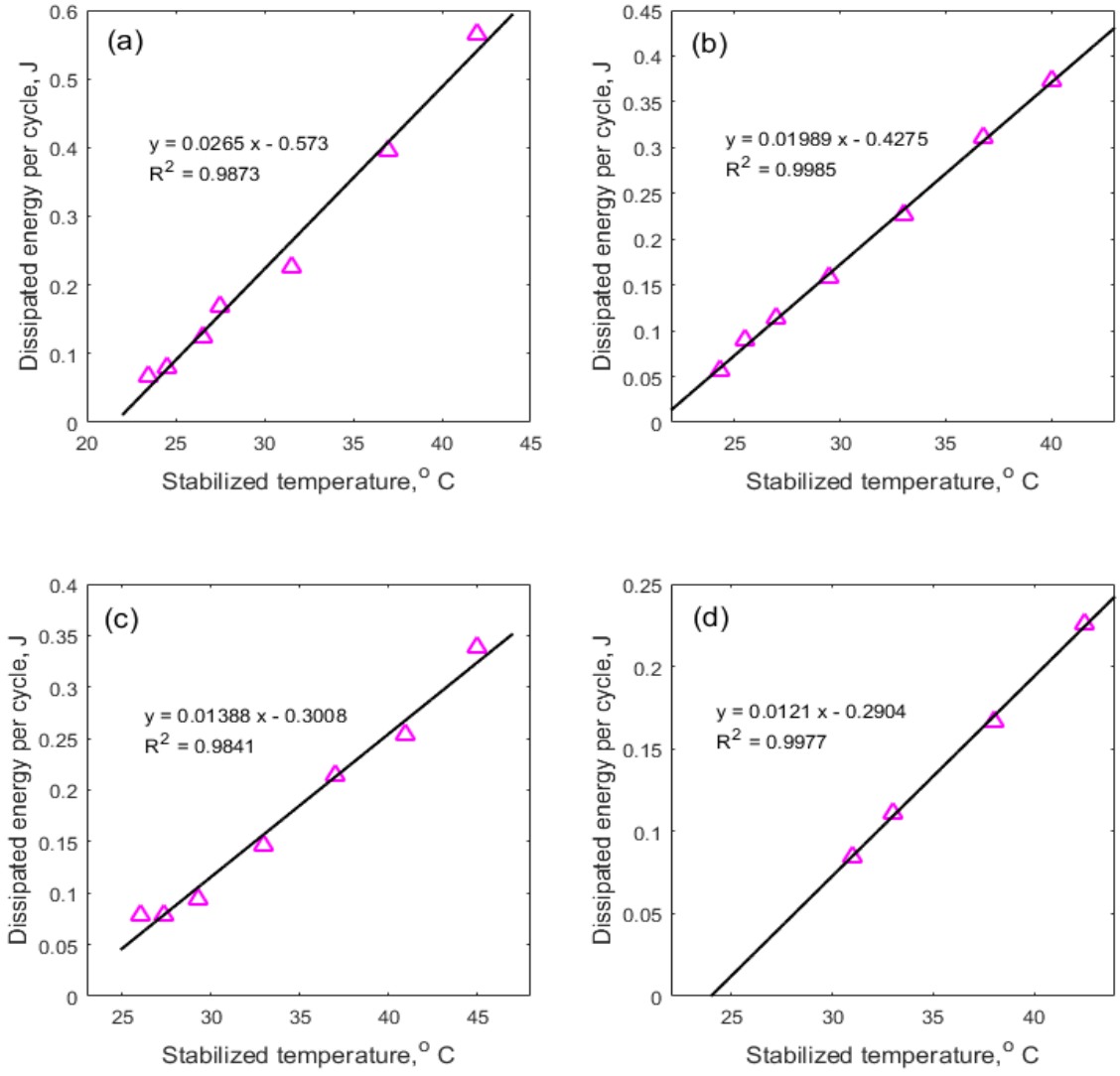

Figure 23: Linear relation between stabilized temperature and dissipated energy per cycle at (a) loading frequency = 5 Hz, (b) loading frequency = 7Hz, (c) loading frequency = 10 Hz, (d) loading frequency =15 Hz.

3.4. Conclusion

Both thermographic approach and dissipated energy per cycle based approach exhibited that, HCFS of unidirectional flax fiber reinforced polymer matrix composites changes from 45% load of UTS to 40% load of UTS due to change of loading frequency from 5 Hz to 15 Hz. As expected, HCFS decreases with increasing loading frequency, but the amount of decrease is little compared to the change of loading frequency. Furthermore, for same percentages of applied

stresses, dissipated energy per cycle does not change with changing loading frequency. However, for same percentages of applied stress, sample surface temperature shows significant increase with increasing loading frequency. These thermal degradation due to high sample temperature at higher loading frequency may play a significant to decrease HCFS at higher loading frequency. Material which is not continuously loaded with higher loading frequency may not encounter thermal degradation in real life application. Therefore, effect of loading frequency on HCFS would be more insignificant if thermal degradation of sample could be separated from the fatigue damage. Knowledge about HCFS of flax fiber reinforced composites at higher loading frequency may create an era of using flax fiber reinforced composites under high frequency cyclic loading.

4. SEPARATION OF ENERGY COMPONENT (SELF-HEATING AND DAMAGE) DURING CYCLIC LOADING OF FLAX FIBER REINFORCED COMPOSITES

4.1. Introduction

Natural fiber reinforced composites heats up significantly during cyclic loading due to the low thermal conductivity of natural fibers. However, due to the thermal balance between heat generated within the sample and the heat transferred from the sample to the surrounding, the sample temperature reaches to a stable value after a few initial fatigue cycles. As a sample of natural fiber reinforced composites (NFRC) heats up significantly during the testing under fatigue loading, the progression of the overall fatigue damage within the NFRC occurs due to two forms of damage; thermal damage due to the self-heating of the sample and micro-mechanical damage due to the repetitive loading and unloading [45].

The fatigue life of composite materials decreases with increasing loading frequency [39, 41]. Hence, the overall fatigue damage within the sample increases with loading frequency. Moreover, self-heating temperature or thermal degradation of the sample also increases with the loading frequency of the fatigue test [41]. However, real life structural materials encountered cyclic loading intermittently at higher loading frequencies may not have to encounter thermal degradation as those members will have sufficient time to transfer the heat generated. Therefore, the micro-mechanical damage is the only damage component that will work to create the fatigue damage at higher loading frequencies within the intermittently loaded structural components. A method for separating the overall fatigue damage energy into thermal and micro-mechanical damage component was proposed and successfully implemented by Meneghetti for steel and short fiber reinforced composites [33, 34, 46]. The effect of loading frequency on the micro-mechanical damage creation due to repetitive loading and unloading is not well understood. Therefore, the

overall goal of this study was to separate the contribution of thermal damage and micro-mechanical damage in order to define how fatigue life of flax fiber reinforced composites decrease with increasing loading frequency.

4.2. Theory

During the loading portion of the fatigue testing, the sample absorbs energy and during the unloading portions the sample releases the energy. The difference in those two energies is the total dissipated energy (E_T) during fatigue cycling. The area under the stress-strain curve represents the E_T, which can be determined by using Equation (7) and Equation (8).

$$E_T(per\ unit\ time) = \frac{(\oint F\ ds)}{V} \times f \tag{7}$$

$$E_T(per\ cycle) = \frac{(\oint F\ ds)}{V} \tag{8}$$

One portion of the total dissipated energy creates heat in the material and the other portion is responsible for creating micro-mechanical damage within the sample (E_d) [33]. Heat energy generated within the sample will be either transferred by the process of conduction, convection, and radiation ($H_{cd+cv+ir}$) or stored to increase the temperature of the sample ($\rho c \frac{dT}{dt}$) [47, 48]. The distribution of the total dissipated energy is shown in Equation (9).

$$E_T = H_{cd+cv+ir} + E_d + \rho c \frac{dT}{dt} \tag{9}$$

Heat energy transferred to the surrounding ($H_{cd+cv+ir}$) is dependent on the temperature of the sample. The sample temperature becomes stabilized whenever the temperature of the sample reaches a certain value where the heat energy generated within the sample per unit time equals the heat energy transferred to the surroundings per unit time. After the sample temperature reaches a

stable value during fatigue testing, $\frac{dT}{dt} = 0$. Therefore, when the sample temperature is stabilized, Equation (9) will be:

$$E_T = H_{cd+cv+ir} + E_d \tag{10}$$

If the fatigue test is stopped suddenly at a certain time $t = t^*$, when the surface temperature of the sample reaches to a stable value (Figure *24*), then the total dissipated energy within the sample will become zero ($E_T = 0$, as fatigue test stopped) and no damage will accumulate within the sample ($E_d = 0$). However, the temperature of the sample will start to decease with time. Therefore the equation (9) will be as follow [33]–

$$H_{cd+cv+ir} = -\rho c \frac{dT}{dt} \tag{11}$$

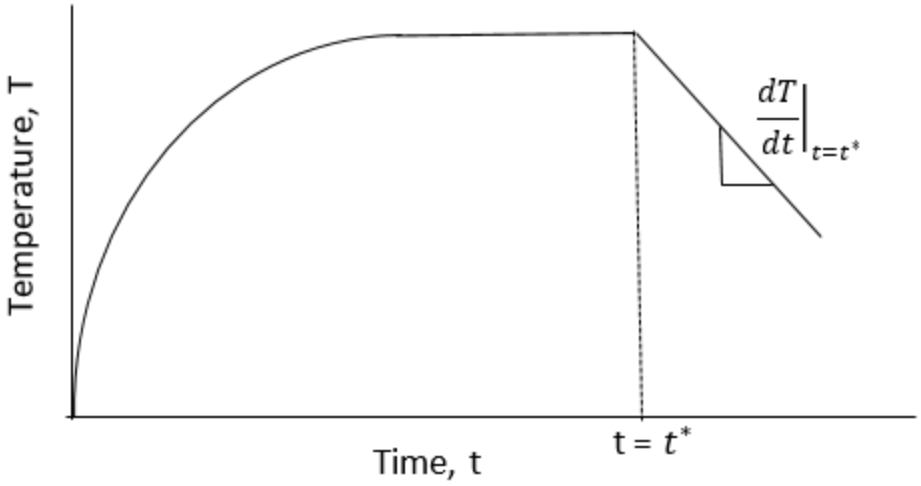

Figure 24: Schematic of the cooling curve of the fatigue sample after stopping the test during stabilized surface temperature of the sample.

After sample temperature reaches a stable value, total heat energy ($H_{cd+cv+ir}$) transferred from the sample by conduction, convection, and radiation is possible to determine easily by using Equation (11). Moreover, energy responsible to create micro-mechanical damage within the sample (E_{d}) is possible to determine by rearranging equation (10) as follow-

$$E_d = E_T - H_{cd+cv+ir} \quad (12)$$

4.3. Materials and methods

As discussed in section 3.2, Samples for fatigue testing of unidirectional flax fiber reinforced composites were cut down from a panel produced by vacuum assisted resin transfer molding (VARTM). Non-crimp unidirectional flax fiber fabric (105 tex, weft thread = 1/cm, weight =300 gsm) was purchased from BComp amplitex. The Infusion epoxy resin with amide hardener (mixed resin viscosity = 129 cP and density =9.5 lb/gal at 22 ˚C) was used as a matrix materials. Twelve layers of unidirectional flax fiber fabric were used to prepare a panel (12 in. × 12 in.) by VARTM. Post curing was accomplished for 3 days at room temperature and 8 hours at 80 °C. Volume fraction of produced panel of unidirectional flax fiber was about 50%. Produced flax fiber reinforced polymer matrix composites have following properties: Material properties: density, ρ = 1309 kg/m^3, and specific heat, c = 1280.43 J/kg ˚C.

ASTM 3039 standard was followed to cut test samples from the panel prepared by the process of VARTM. The sample size was 10 in. long, 1 in. in width, and 0.18 in. in thickness. Glass fiber tabs of 2.25 in. long were inserted on each side of the sample to ensure better load transfer. Effective length of the sample (5.5 inch) was calculated by subtracting tabs length form the original sample, which was used to calculate the volume of the sample (V). All tensile and fatigue tests were accomplished using MTS 250 kN servo-hydraulic load frame. Tensile testing was completed to obtain information about the ultimate tensile strength (UTS) of the materials. Fatigue tests were conducted at 50% load of the ultimate tensile strength of the materials. Load variation during fatigue/cyclic loading was sinusoidal. Minimum applied stress during fatigue loading was 10% of the maximum applied stress which is defined as loading ratio, R = 0.1.

Fatigue test were conducted at 50% load of UTS for the loading frequencies of 5, 7, 10, and 15 Hz. Due to viscoelastic nature of natural fiber and resin, the sample become heated significantly during cyclic loading. An IR camera was used to capture the temperature distribution of the sample during cyclic loading. Fatigue testing was stopped whenever the temperature of the sample was stabilized. Just after stopping the test, the cooling rate of the sample was also measured by using a thermal IR camera. To determine the dissipated energy per fatigue cycle force and elongation data was captured during cyclic loading with a data acquisition frequency that endure around 102 data point per fatigue cycle.

4.4. Results

Fatigue testing was conducted at the 50% load of UTS for the loading frequencies of 5, 7, 10, and 15 Hz. In section 3.3.1, Figure 18 exhibited the temperature distribution of the sample tested at different loading frequency. Temperature of the sample stabilized after a certain number of cycle. The stabilized sample temperature increased significantly with increasing loading frequency. In section 3.3.2, Figure 20 showed the distribution of total dissipated energy per cycle (E_T) during the cyclic loading at different loading frequency. The area enclosed by hysteresis loop (load-elongation diagram) represent the total dissipated energy per cycle. Total dissipated energy per cycle does not change significantly with loading frequency (ANOVA tested, section 3.3.2). Although stabilized surface temperature of the sample increased significantly with increasing loading frequency, total dissipated energy per fatigue cycle do not change significantly with loading frequency.

Figure 25 shows the cooling curves of the samples just after stopping the fatigue tests whenever the temperature of the sample become stabilized (at time t =t^*). Slope of the cooling curve represents cooling rate ($\frac{dT}{dt}$)

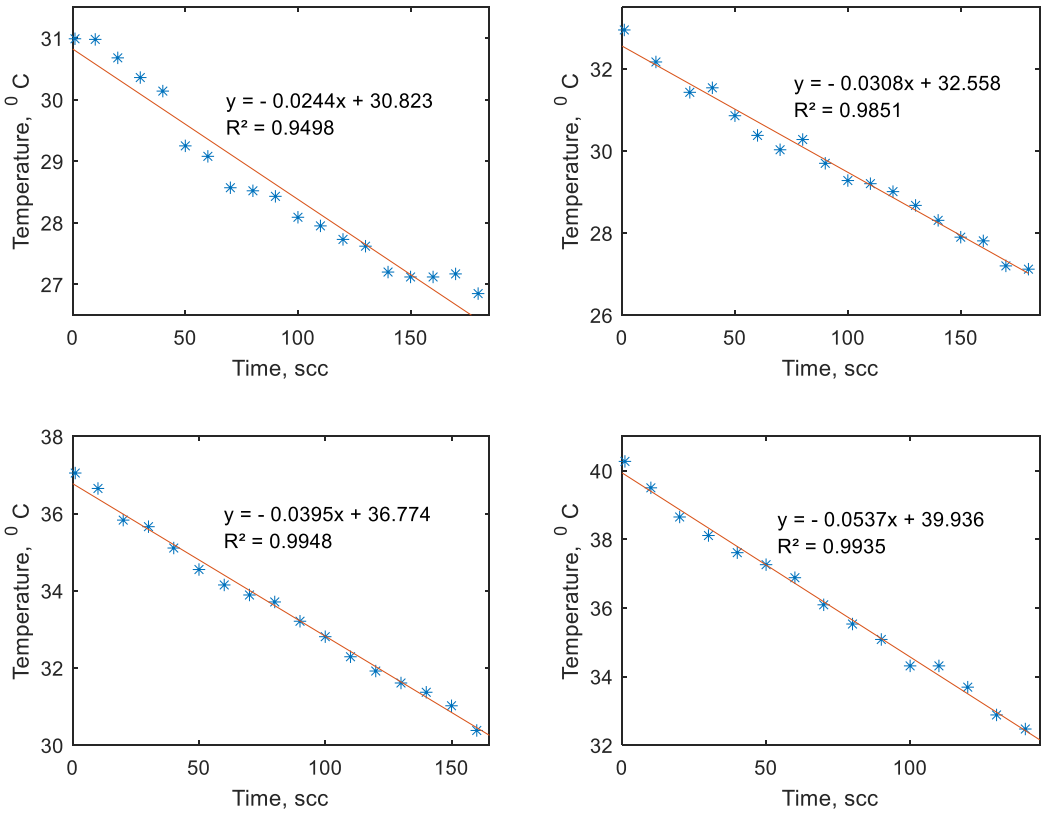

Figure 25: Cooling curve of the sample after stopping the fatigue test during stabilized sample temperature at 50% load of UTS for the (a) loading frequency = 5 Hz, (b) loading frequency =7 Hz, (c) loading frequency = 10 Hz, and (d) loading frequency = 15 Hz.

Cooling rate $\left(\frac{dT}{dt}\right)$ was calculated from Figure 25 by measuring the slope of the cooling curve at time t=0. Cooling rate for different loading frequency (f) are as follow-

$$\frac{dT}{dt}(f = 5\ Hz) = -0.0244$$

$$\frac{dT}{dt}(f = 7\ Hz) = -0.0308$$

$$\frac{dT}{dt}(f = 10\ Hz) = -0.0395$$

$$\frac{dT}{dt}(f = 15\ Hz) = -0.0537$$

Table 9 exhibited the separation of the total dissipated energy per unit time into the heat energy generated within the sample per unit time and the energy responsible for the damage creation within the sample per unit time. As shown in Figure 26 (b), heat energy generated within the sample per unit time increases linearly with loading frequency. Moreover, heat energy transfer from the sample to the surroundings per unit time is a function of the temperature of the sample. More heat transfer will happen at higher sample temperature. Therefore, the thermal balance between the generated heat energy due to cyclic loading and transferred heat energy from the sample will be happening at higher temperature during the fatigue test at higher loading frequency. Hence, the stabilized surface temperature of the sample also increases linearly with increasing loading frequency (Figure 26 (a)). These higher sample temperatures cause high thermal degradation of the sample during the fatigue test at higher loading frequency. Hence fatigue damage due to thermal degradation should increase linearly with the loading frequency.

Table 10 shows the separation of the total dissipated energy in one single fatigue cycle into the heat energy generated within the sample in one single fatigue cycle and the energy responsible for the damage creation within the sample in one single fatigue cycle. It is vivid from Table 10 that, both heat energy and damage creation energy per fatigue cycle does not change much with loading frequency. As thermal degradation happen due to higher sample temperature during cyclic loading, the heat energy is therefore the main responsible form of energy for the variation of fatigue life due to the change of the loading frequency.

Table 9: Separation of Total Dissipated Energy (per Unit Time) During Cyclic Loading.

	Total dissipated energy (per unit time), J/(m^3.sec)	Heat energy (per unit time), J/(m^3.sec)	Energy for damage creation (per unit time), J/(m^3.sec)
5 Hz	75848	40896	34952
7 Hz	96534	51623	44911
10 Hz	131694	66205	65488
15 Hz	207938	90005	117933

Table 10: Separation of Total Dissipated Energy (per Cycle) During Cyclic Loading.

	Total dissipated energy (per fatigue cycle), J/(m^3.cycle)	Heat energy (per fatigue cycle), J/(m^3.cycle)	Energy for damage creation (per fatigue cycle), J/(m^3.cycle)
5 Hz	15169	8179	6990
7 Hz	13790	7374	6415
10 Hz	13169	6620	6548
15 Hz	13862	6000	7862

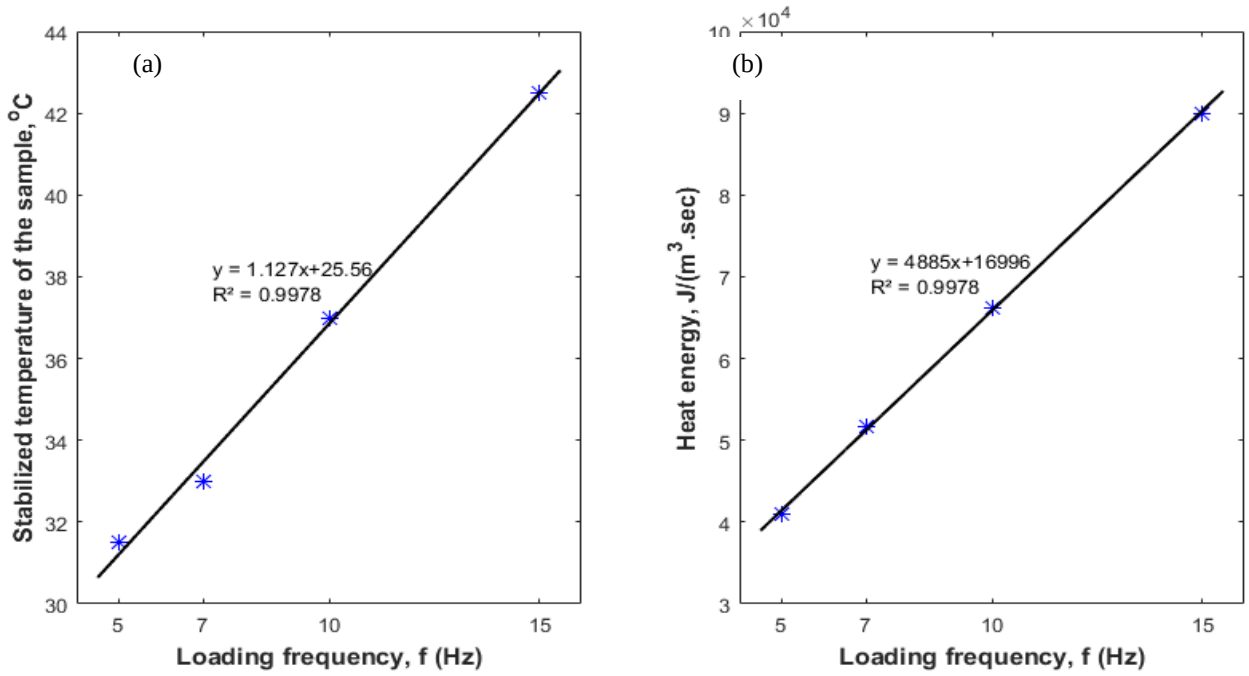

Figure 26: Linear relation between stabilized surface temperature and (a) loading frequency (b) heat energy generated within the sample per unit time.

4.5. Conclusion

Because of the high thermal degradation of the samples at higher loading frequency, fatigue life of flax fiber reinforced composites decrease with increasing loading frequency. Heat energy generated per unit time within the sample increases linearly with loading frequency. Due to low thermal conductivity of flax fiber reinforced composites, this generated heat energy make the sample temperature high. However, micro-mechanical damage creation per fatigue cycle due to cyclic loading does not vary significantly with increasing loading frequency. Therefore, if thermal degradation is not considered, fatigue life of flax fiber reinforced composites may not vary significantly with increasing loading frequency. A structural member encountered intermittent or infrequent cyclic loading at higher frequency might have substantial time to release generated heat energy. Therefore, fatigue life may not vary with loading frequency for a member loaded with intermittent or infrequent cyclic loading. As thermal degradation is mainly responsible for

decreasing fatigue life at higher loading frequency, it is therefore expected a fatigue test conducted at lower loading frequency but higher ambient temperature would also show a decrease in fatigue life/fatigue limit due to high thermal degradation.

5. CONCLUSION AND FUTURE RECOMMENDATIONS

Flax fiber reinforced polymer matrix composites exhibit excellent properties under cyclic loading. Mathematical modeling, self-hating temperature based thermographic approach, and dissipated energy per cycle based approaches estimates the fatigue limit of unidirectional flax fiber reinforced composites is about 45% load of UTS at a loading frequency of 5 Hz. Similar fatigue limit was also reported in literature for unidirectional flax fiber reinforced composites by performing full fatigue test and thermographic approach [10]. Moreover, thermographic and dissipated energy per cycle based approaches was accomplished at different loading frequencies (5, 7, 10, and 15 Hz) and showed the fatigue limit does not change much with changing loading frequencies. Fatigue limit changes from 45% load of UTS to 40% load of UTS with the loading frequency changes from 5 Hz to 15 Hz. Although self-heating temperature of sample during cyclic loading increases significantly with increasing loading frequency, total dissipated energy per cycle does not changes significantly with increasing loading frequency.

Fatigue damage of flax fiber reinforced polymer matrix composites occurs due the combination of thermal damage due to self-heating of the sample and micromechanical damage (crack initiation, crack propagation) creation due to repetitive loading. Those two damage components were experimentally separated to define their individual effect on fatigue life. The thermal damage and self-heating temperature of the sample tested under fatigue loading increases linearly with loading frequency. Micromechanical damage creation per cycle due to cyclic loading does not change much with loading frequency. Therefore, the thermal damage is the main form of damage energy responsible for decreasing fatigue life with increasing loading frequency.

Performing fatigue test at high ambient temperature and low loading frequency can also verify the effect of thermal damage on the fatigue life of flax fiber reinforced composites. Fatigue

limit of bio-based flax fiber reinforced polymer matrix composites can be further increased by laminating. Furthermore, hybridization with synthetic fiber can also increase the fatigue limit of bio-based flax fiber reinforced polymer matrix composites. Damage propagation mechanism and rate of damage propagation through flax fiber reinforced composites is not well understood. Thermographic and acoustic emission measurement was used in literature to understand damage propagation through synthetic fiber reinforced polymer matrix composites. Using those approaches to define damage propagation mechanism through flax fiber reinforced composites may open new possibilities to develop self-healing flax fiber reinforced composites. Furthermore, knowledge about damage propagation mechanism should play an important role while choose proper lamination of composites for specific applications.

REFERENCES

[1] M. Haggui, A. El Mahi, Z. Jendli, A. Akrout, M. Haddar, Static and fatigue characterization of flax fiber reinforced thermoplastic composites by acoustic emission, Applied acoustics 147 (2019) 100-110.

[2] A. Warhadpande, B. Jalalahmadi, T. Slack, F. Sadeghi, A new finite element fatigue modeling approach for life scatter in tensile steel specimens, International Journal of Fatigue 32(4) (2010) 685-697.

[3] H. Mao, S. Mahadevan, Fatigue damage modelling of composite materials, Composite Structures 58(4) (2002) 405-410.

[4] M. Kaminski, F. Laurin, J. Maire, C. Rakotoarisoa, E. Hémon, Fatigue damage modeling of composite structures: the onera viewpoint, AerospaceLab (9) (2015) p. 1-12.

[5] L. Toubal, M. Karama, B. Lorrain, Damage evolution and infrared thermography in woven composite laminates under fatigue loading, International journal of Fatigue 28(12) (2006) 1867-1872.

[6] F. Bensadoun, K. Vallons, L.B. Lessard, I. Verpoest, A. Van Vuure, Fatigue behaviour assessment of flax–epoxy composites, Composites Part A: Applied Science and Manufacturing 82 (2016) 253-266.

[7] A. Shahzad, Investigation into fatigue strength of natural/synthetic fiber-based composite materials, Mechanical and Physical Testing of Biocomposites, Fibre-Reinforced Composites and Hybrid Composites, Elsevier2019, pp. 215-239.

[8] J. Gassan, A study of fibre and interface parameters affecting the fatigue behaviour of natural fibre composites, Composites part A: applied science and manufacturing 33(3) (2002) 369-374.

[9] D.U. Shah, P.J. Schubel, M.J. Clifford, P. Licence, Fatigue life evaluation of aligned plant fibre composites through S–N curves and constant-life diagrams, Composites Science and Technology 74 (2013) 139-149.

[10] I. El Sawi, Z. Fawaz, R. Zitoune, H. Bougherara, An investigation of the damage mechanisms and fatigue life diagrams of flax fiber-reinforced polymer laminates, Journal of materials science 49(5) (2014) 2338-2346.

[11] T. Jeannin, X. Gabrion, E. Ramasso, V. Placet, About the fatigue endurance of unidirectional flax-epoxy composite laminates, Composites Part B: Engineering 165 (2019) 690-701.

[12] X. Zhao, X. Wang, Z. Wu, T. Keller, A.P. Vassilopoulos, Effect of stress ratios on tension–tension fatigue behavior and micro-damage evolution of basalt fiber-reinforced epoxy polymer composites, Journal of materials science 53(13) (2018) 9545-9556.

[13] P.R. Vieira, E.M.L. Carvalho, J.D. Vieira, R.D. Toledo Filho, Experimental fatigue behavior of pultruded glass fibre reinforced polymer composite materials, Composites Part B: Engineering 146 (2018) 69-75.

[14] S. Liang, P.-B. Gning, L. Guillaumat, A comparative study of fatigue behaviour of flax/epoxy and glass/epoxy composites, Composites Science and Technology 72(5) (2012) 535-543.

[15] Y. Ueki, H. Lilholt, B. Madsen, Fatigue behaviour of uni-directional flax fibre/epoxy composites, 20th International Conference on Composite Materials (ICCM20), ICCM20 Secretariat, 2015.

[16] D.U. Shah, Damage in biocomposites: Stiffness evolution of aligned plant fibre composites during monotonic and cyclic fatigue loading, Composites Part A: Applied Science and Manufacturing 83 (2016) 160-168.

[17] G. La Rosa, A. Risitano, Thermographic methodology for rapid determination of the fatigue limit of materials and mechanical components, International journal of fatigue 22(1) (2000) 65-73.

[18] G. Fargione, A. Geraci, G. La Rosa, A. Risitano, Rapid determination of the fatigue curve by the thermographic method, International journal of fatigue 24(1) (2002) 11-19.

[19] J. Montesano, Z. Fawaz, H. Bougherara, Use of infrared thermography to investigate the fatigue behavior of a carbon fiber reinforced polymer composite, Composite structures 97 (2013) 76-83.

[20] J. Huang, M. Pastor, C. Garnier, X. Gong, A new model for fatigue life prediction based on infrared thermography and degradation process for CFRP composite laminates, International Journal of Fatigue 120 (2019) 87-95.

[21] C. Peyrac, T. Jollivet, N. Leray, F. Lefebvre, O. Westphal, L. Gornet, Self-heating method for fatigue limit determination on thermoplastic composites, Procedia Engineering 133 (2015) 129-135.

[22] R. Prochazka, J. Dzugan, P. Konopik, Fatigue limit evaluation of structure materials based on thermographic analysis, Procedia Structural Integrity 7 (2017) 315-320.

[23] ASTM D3039: Standard Test Method for Tensile Properties of Polymer Matrix, ASTM.

[24] ASTM D3479: Standard Test Method for Tensiontension Fatigue Or Polymer Matrix, ASTM.

[25] C. Poilâne, Z. Cherif, F. Richard, A. Vivet, B.B. Doudou, J. Chen, Polymer reinforced by flax fibres as a viscoelastoplastic material, Composite Structures 112 (2014) 100-112.

[26] C. Poilâne, F. Gehring, H. Yang, F. Richard, About Nonlinear Behavior of Unidirectional Plant Fibre Composite, Advances in Natural Fibre Composites, Springer2018, pp. 69-79.

[27] S. Ahmed, C. Ulven, Dynamic in-situ observation on the failure mechanism of flax fiber through scanning electron microscopy, Fibers 6(1) (2018) 17.

[28] R. Chandra, S. Singh, K. Gupta, A study of damping in fiber-reinforced composites, Journal of Sound and Vibration 262(3) (2003) 475-496.

[29] F. Lahuerta, R.P. Nijssen, Energy dissipation in thermoset composites in mode I fatigue, Mechanics of Advanced Materials and Structures 24(2) (2017) 168-175.

[30 S. Zhu, M. Mizuno, Y. Kagawa, Y. Mutoh, Monotonic tension, fatigue and creep behavior of SiC-fiber-reinforced SiC-matrix composites: a review, Composites Science and Technology 59(6) (1999) 833-851.

[31] A. Katunin, Domination of self-heating effect during fatigue of polymeric composites, Procedia Structural Integrity 5 (2017) 93-98.

[32] J. Kaleta, R. Blotny, H. Harig, Energy stored in a specimen under fatigue limit loading conditions, Journal of testing and evaluation 19(4) (1991) 326-333.

[33] G. Meneghetti, Analysis of the fatigue strength of a stainless steel based on the energy dissipation, International journal of fatigue 29(1) (2007) 81-94.

[34] G. Meneghetti, M. Quaresimin, M. De Monte, Fatigue strength assessment of a short fibre-reinforced plastic based on the energy dissipation, Proceedings of the 16th International Conference on Composite Materials, 2007.

[35] Q. Guo, X. Guo, J. Fan, R. Syed, C. Wu, An energy method for rapid evaluation of high-cycle fatigue parameters based on intrinsic dissipation, International Journal of Fatigue 80 (2015) 136-144.

[36] Y. Duan, J.A. Griggs, Effect of loading frequency on cyclic fatigue lifetime of a standard-diameter implant with an internal abutment connection, Dental Materials 34(12) (2018) 1711-1716.

[37] H. Mayer, M. Papakyriacou, R. Pippan, S. Stanzl-Tschegg, Influence of loading frequency on the high cycle fatigue properties of AlZnMgCu1. 5 aluminium alloy, Materials Science and Engineering: A 314(1-2) (2001) 48-54.

[38] I. Marines, G. Dominguez, G. Baudry, J.-F. Vittori, S. Rathery, J.-P. Doucet, C. Bathias, Ultrasonic fatigue tests on bearing steel AISI-SAE 52100 at frequency of 20 and 30 kHz, International Journal of Fatigue 25(9-11) (2003) 1037-1046.

[39] J. Dally, L. Broutman, Frequency effects on the fatigue of glass reinforced plastics, Journal of Composite Materials 1(4) (1967) 424-442.

[40] D. Curtis, D. Moore, B. Slater, N. Zahlan, Fatigue testing of multi-angle laminates of CF/PEEK, Composites Evaluation, Elsevier1987, pp. 40-50.

[41] R. Růžek, M. Kadlec, L. Petrusová, Effect of fatigue loading rate on lifespan and temperature of tailored blank C/PPS thermoplastic composite, International Journal of Fatigue 113 (2018) 253-263.

[42] D.V.O. de Moraes, R. Magnabosco, G.H.B. Donato, S.H.P. Bettini, M.C. Antunes, Influence of loading frequency on the fatigue behaviour of coir fibre reinforced PP composite, Polymer Testing 41 (2015) 184-190.

[43] C. Sun, W. Chan, Frequency effect on the fatigue life of a laminated composite, Composite materials: testing and design (fifth conference), ASTM International, 1979.

[44] F.K. Sodoke, L. Toubal, L. Laperrière, Hygrothermal effects on fatigue behavior of quasi-isotropic flax/epoxy composites using principal component analysis, Journal of materials science 51(24) (2016) 10793-10805.

[45] D. Lei, P. Zhang, J. He, P. Bai, F. Zhu, Fatigue life prediction method of concrete based on energy dissipation, Construction and Building Materials 145 (2017) 419-425.

[46] G. Meneghetti, M. Ricotta, The Dissipated Heat Energy as a Fatigue Damage Index For Experimental Fatigue Life Estimations, Procedia engineering 213 (2018) 313-322.

[47] M. Naderi, A. Kahirdeh, M. Khonsari, Dissipated thermal energy and damage evolution of Glass/Epoxy using infrared thermography and acoustic emission, Composites Part B: Engineering 43(3) (2012) 1613-1620.

[48] M. Naderi, M. Khonsari, On the role of damage energy in the fatigue degradation characterization of a composite laminate, Composites Part B: Engineering 45(1) (2013) 528-537.